UNIVERSITY OF TURKU

Selection and characterization of DARPins against therapeutically relevant target proteins

Master's thesis

Department of Biotechnology

Biomolecular production

April 2025

Paulus Nyman

Master's thesis

Subject: Selection and characterization of DARPins against therapeutically relevant target proteins
Author: Paulus Nyman
Title: BSc (tech)
Supervisors: PhD Bryce Nelson, PhD Ralf Paul, PhD Tuomas Huovinen
Number of pages: 57 pages
Date: 27.3.2025

DARPins (designed ankyrin repeat proteins) are small non-antibody binders. Their stability, high expression in prokaryotic cells, and lack of disulfide bridges make them interesting research topic for therapeutic and diagnostic use.

In this study, a previously constructed DARPin library was screened against two target proteins with clinical significance (undisclosed, referred as X and Y). Phage display biopanning was used for isolating binders. The enrichment of binders was confirmed with phage immunoassay from total panning output and from individual clones. With four panning rounds, >50 % hit rate against X and >15 % against Y were achieved, when signal to background ratios over three were counted as hit. The best binders against X and Y showed S/B ratios over 400 and 250, respectively. That confirmed the success of selections. To create even stronger binders against target Y, DARPins from fourth round were combined with peptide linkers of multiple lengths. New bivalent library was screened with off-rate panning to select the strongest binders. Individual DARPins showing the highest binding in immunoassay were produced and the binding was characterized. Best binders for both X and Y had affinities in nanomolar range (<10 nM).

Afterwards, validated binders could be taken into further development such as screened for functional properties against the target proteins. At this state, the study has proven the effectiveness of used library and methods for binder discovery, even against potentially challenging proteins. In the future, the pipeline could be used as a platform for early-stage drug development for multiple different targets.

Key words: binder, biopanning, DARPin, drug development, epitope, phage display

Table of contents

Abbreviations

ADC	Antibody-Drug Conjugate
AR2G	Amine Reactive 2nd Generation biosensor for Octet
ATP	Adenosine Triphosphate
BLI	Biolayer Interferometry
BSA	Bovine Serum Albumin
CAR-T cell	Chimeric Antigen Receptor T cell
CFU	Colony Forming Unit, the number of individual cells or viruses
DARPin	Designed Ankyrin Repeat Protein
DBCO	Dibenzocyclooctyne, a compound used in chemical linking
DELFIA	Dissociation-Enhanced Lanthanide Fluorescent Immunoassay
DDM	n-Dodecyl β-D-Maltoside
DNA	Deoxyribonucleic Acid
DTT	Dithiothreitol
EDC	1-Ethyl-3-(3-dimethylaminopropyl) carbodiimide
EGFR	Epidermal growth factor receptor
ELISA	Enzyme-Linked Immunosorbent Assay
EU	Europium (label used in immunoassays)
Fab	Fragment Antigen-Binding region
Fc	Fragment Crystallizable (region of antibody)
GST	Glutathione S-Transferase, commonly used as a protein fusion tag
HER2	Human Epidermal Growth Factor Receptor 2
IgG	Immunoglobulin G, a type of antibody
IMAC	Immobilized Metal Affinity Chromatography
IM	Intramuscular (injection route)
IPTG	Isopropyl β-D-1-thiogalactopyranoside
IV	Intravenous (injection route)
KD	Dissociation constant
MMAE	Monomethyl auristatin E, short peptide cytotoxin
MOI	Multiplicity of infection, number viral particles per host cell
MOPS	3-(N-Morpholino)propanesulfonic acid
NEB	New England Biolabs, a supplier of molecular biology reagents
NHS	N-Hydroxysuccinimide
O/N	Overnight, e.g., incubation of bacterial cultures
OD600	Optical Density at 600 nm, typically from bacterial culture
PCR	Polymerase Chain Reaction
PET	Positron Emission Tomography
qPCR	Quantitative Polymerase Chain Reaction
R0	Initial DARPin library used in the study
RT	Room Temperature
S/B	Signal-to-Background ratio
scFv	Single-Chain Variable Fragment (antibody)
SDS-PAGE	Sodium Dodecyl Sulfate-Polyacrylamide Gel Electrophoresis
SPAAC	Strain-Promoted Azide-Alkyne Cycloaddition
SRP	Signal Recognition Particle
TCEP	Tris(2-carboxyethyl)phosphine

1 Introduction

1.1 Drug discovery and protein therapeutics

Modern drug discovery starts from discovering a mechanism and pathway of a certain disease. From a pathway, a target, typically protein such as an enzyme, G-protein coupled receptor, ion channel, or membrane transport protein, is chosen. Target needs to play a critical role in the disease so that altering the function of target with a drug can have an impact as a treatment. Once the target is chosen, the appropriate modality is determined (e.g., small molecule, large molecule, covalent, or non-covalent inhibitor) and a Target Molecule Profile (TMP) is developed. The TMP outlines detailed requirements, including binding affinities, desired functionality, pharmacokinetic properties, and the intended route of administration, which is considered early due to its impact on development. Next step is to discover compounds that interact with the target, either through covalent or non-covalent bonding. Interaction is characterized, compounds with validated desirable function to target are called leads. Biophysical properties such as solubility and stability are further evaluated. (Blass, 2015; Wyatt et al., 2011).

Before approval as a drug, the safety is ensured by extensive testing. Multiple tests with cells and animals are conducted. In phase I or first in human clinical study, the main objective is to ensure the safety of the drug candidate and to determine tolerated dosing. Size of test group is typically blow 100. If no side effects are assumed initially, Phase I is typically conducted with healthy test group. In phase II, the objective leans more heavily into determining the therapeutic effectivity of the drug. Group of over 100 patients is typically used. Different drug dosages are used to find optimal one. If the results are favourable and market landscape stays positive, phase 3 is started with chosen dosage and larger 1000 scale patient group. Proven effectiveness and limited adverse events compared to the benefits can lead into regional approval, and the drug can be sold in the market. (Blass, 2015; Piantadosi, 2024).

Small molecules are the biggest molecule group used as drugs. To achieve high affinity, small molecules often require a hydrophobic pocket in the target, limiting the pool of druggable targets. Molecules are typically found in big libraries by screening in-vitro, computationally or by combining these methods. Due to stability and good tissue

penetration, small molecules can typically be administered orally and the compound reaches the target tissue by diffusion. (Blass, 2015).

Antibody-based therapeutics have become popular over the past decades, market exceeding 200 billion USD in 2023. (MarketsandMarkets, 2024). Antibodies are an example of protein-based therapeutics. They are capable of binding to virtually any target due to their large binding site, paratope, where each amino acid can form multiple non-covalent bonds with a target. Antibodies can be bispecific and they can be linked to different drug molecules, creating antibody drug conjugates, ADCs. (Goulet & Atkins, 2020).

Large size (~150 kDa for IgG) and complex structure of antibodies requires eukaryotic host cells for production and results in relatively low yields. Disulfide-bond containing structure is limited in stability and functions only in extracellular oxidizing conditions. These properties increase the production and storage costs and limit the use cases for antibodies (Plückthun, 2015). Additionally, the patent landscape related to antibody development, production, and utilization is complex, introducing licence and other legal costs.

To tackle the challenges with antibodies, improvements to antibody structure have been made regarding stability, immunogenicity, and pharmacokinetics. Different antibody frameworks have been utilized. Nanobodies are small, single domain antibodies derived from camelids. They are easy to produce recombinantly. Small size also contributes to certain pharmacokinetics, including good tissue penetration. Small and simple structure can be achieved by using scFv (single-chain variable fragment) antibodies, where light and heavy variable chains are linked together, creating one chain with size of ~25 kDa. Fab fragment has more complex structure that is closer to an antibody. In Fab, only Fc region is left out resulting in ~50 kDa protein. (Jin et al., 2023).

Cyclic peptides are a wide group of small (0.5-2.5 kDa) proteins that differ from antibodies structurally and conceptually. There is no constant region and most of the amino acids participate in binding the target molecule. The group includes compounds in therapeutic uses such as hormones (oxytocin) and antibiotics (vancomycin). While most cyclic peptide therapeutics target extracellularly, some of them in development are capable of crossing the cell membrane. Due to cyclic structure, the peptides are typically produced in cells using non-ribosomal synthesis. They can also be fully synthesized

chemically. These methods allow using non-natural amino acids, outside the 20 amino acids that are not used in ribosomal protein synthesis, further diversifying the possible structures. For library selection, most short peptides can be displayed by ribosomal translation utilizing methods such as ribosome or phage display (principles explained in chapter: 1.4. Display methods). Unless the cyclic structure is inherently formed through disulfide bonds between cysteine residues, cyclization can be induced chemically after translation. (Cary et al., 2017; Ji et al., 2024).

Another approach are alternative scaffold binder proteins, where the structure is not related to antibodies. The general concept is still the same, protein consists of constant amino acids providing the base structure and variable amino acids contributing to the binding reaction. One promising group of alternative scaffold proteins are Designed Ankyrin Repeat Proteins, DARPins.

1.2 DARPins

1.2.1 Ankyrin repeat

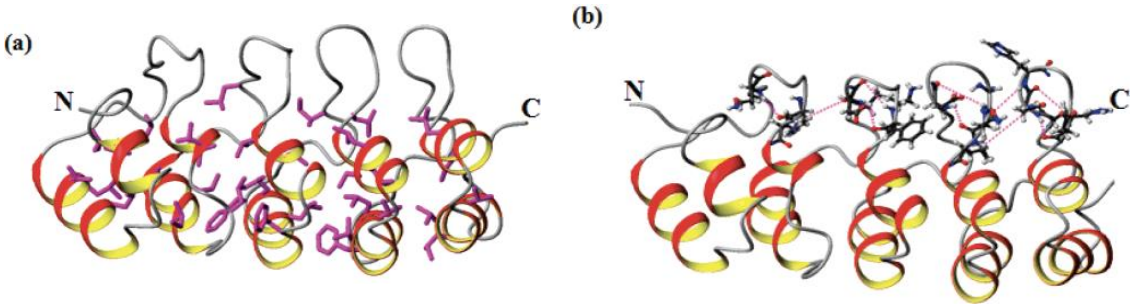

Figure 1. Example 3D model of an ankyrin repeat protein explains the stability of cysteine-free structure. P18 (PDB entry 1BU9) is a protein responsible for regulating the cell cycle by inhibiting human CDK4 receptor. (a) Side chains of residues constituting the hydrophobic core of p18 protein are coloured magenta. (b) The hydrogen bonding network of p18 in its alpha-sheets is coloured magenta. From Li et al., 2006.

Ankyrin repeat is one of the most common protein structures in eukaryotes and viruses, participating in various physiological processes in cells which involve protein-protein binding. The protein consist consists of multiple motifs formed by 30-34 amino acid in helix-turn-helix conformation. Cross-bonding amino acids in tertiary structure are relatively close also in primary sequence, simplifying the folding process. No disulfide bonds are found on the structure; the generally beneficial bond regarding stability would only form outside cell cytoplasm and could be problematic in protein engineering. The

tertiary structure protein is stabile regardless, due to various noncovalent interactions between helixes (Figure 1). (Li et al., 2006).

1.2.2 Development of DARPins

Designed Ankyrin Repeat Proteins are developed based on ankyrin repeat. The general idea (Figure 2) is to have modular binder with the possibility to change the number or order of the repeats. Deriving the structure from naturally occurring proteins potentially reduces unwanted immunoreactions from patient in therapeutic use (Binz et al., 2003).

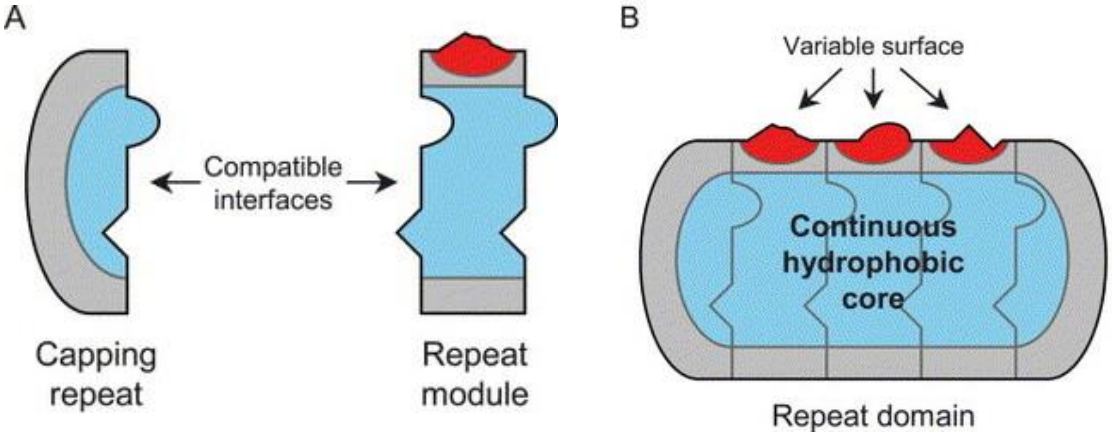

Figure 2. Idea behind DARPins. (A) Repeat module contains variable amino acids and forms the binding surface. Compatible interfaces form hydrophobic interactions, stabilizing the structure. Capping repeat provides hydrophilic surface at the ends of the protein, further stabilizing the structure and improving the physical properties. (B) Compatible building blocks offer flexibility to determine the size of a binder, maintaining continuous binding surface. From: Forrer et al., 2003

1.2.3 DARPin characteristics

DARPins are relatively small (14−18 kDa), easy folding proteins that have a stable, monomeric, cysteine free structure. They can be produced in prokaryotic cells and are functional even in reducing intracellular conditions. These properties make them an interesting research topic for drug development (M. T. Stumpp et al., 2008).

Structurally, DARPins consist of N-cap, C-cap, and one or more repeats in between with repeating amino acid sequences. Each repeat module contains 6 – 7 variable amino acids, depending on the design. The number of repeat modules can be increased, improving the stability of the protein. Size of the binding site and number of variable amino acids is simultaneously increased, potentially improving the binding capacity. As a downside, the

size of a library to cover all the possible variants increases exponentially with each additional variable amino acid (Park & Cochran, 2010).

DARPins can be further developed. As an example, loop-DARPins have expanded binding surface that allows higher affinities and wider range of targets. That was achieved by changing the variable part in a middle repeat into a loop form, increasing the number of amino acids. Loop form makes the binding site flexible and convex, opposite of typical DARPins with concave binding site, improving the binding properties to picomolar range (Schilling et al., 2014).

Two or more DARPins can easily be linked together using protein linkers and standard protein engineering methods (Verdino et al., 2018). Affinity tags can easily be added or other molecules conjugated. Small side and simple structure allow production of DARPins in *E. coli*. Yields of 200 mg/l can be achieved and purification step is simple due to high stability (M. T. Stumpp et al., 2008).

1.3 Applications of DARPins

1.3.1 Research and diagnostics

Versatility and makes DARPins suitable for research and diagnostic use. They could be used in ELISA type in-vitro diagnostic tests, replacing antibodies. Efficient production could lower the cost making fast testing even more affordable and thus accessible globally. Utilising DARPins in place of antibodies in in-vitro diagnostics could improve test accuracy and specificity.

Another use is as biosensors (Plückthun, 2015). Functional intracellular biosensor systems have been demonstrated (Kummer et al., 2013). Specific binding allows using labelled DARPins in biomedical imaging such as PET (Vorobyeva et al., 2019). In research purposes, many types of binders are utilized. DARPins have been used as crystallization agents for otherwise challenging proteins for X-ray crystallography. (Sennhauser & Grütter, 2008)

1.3.2 DARPins as therapeutics

Easy modifications and versatility of DARPins enable use cases like antibodies and beyond. In therapeutic use, individual DARPins can have functional effect inhibiting,

neutralizing or activating various targets such as enzymes, receptors or proteins in signalling pathways. Unlike antibodies, use of DARPins are not limited to extracellular targets (Amstutz et al., 2005; Verdurmen et al., 2015).

Virtually all the current protein-based therapeutics are administered by injection intravenously (IV), subcutaneously (SC) or intramuscularly (IM). Proteolytic nature of human digestive system typically prevents oral administration, a typical route for small molecule drugs (Vugmeyster et al., 2012). Due to stability and easy availability in gram scale, other administration routes could be worth testing with DARPins (M. T. Stumpp et al., 2008). Recently, oral administration has been demonstrated in mice with stability optimized DARPins (Simeon et al., 2021).

DARPins have been engineered against acute allergic reactions. Most severe of them is anaphylaxis, a potentially fatal condition triggered by certain food or drug molecule causing rapid increase in histamine and other allergy-related mediators. Adrenaline injection is mostly used acute treatment, but it only alleviates acute symptoms such as breathing difficulties without reducing the allergic reaction. IgE antibody is mostly responsible for the initial recognition of antigen, and it binds to FcεRI receptor with high affinity. Pennington's research team selected DARPins against IgE to act as noncompetitive inhibitors. It successfully prevented IgE binding and removed already bound antibody from the receptor, dissociation of the complex would normally be slow. By affinity maturation and rational linking of three DARPins together, inhibition properties were demonstrated, significantly better than antibody reference, omalizumab. Termination of signalling was tested in human blood cells and supressing allergic reaction was demonstrated in mice. (Kim et al., 2012; Pennington et al., 2021).

1.3.3 DARPin drug conjugates

Antibody drug conjugates (ADCs) have demonstrated success in research, clinical testing and as approved drugs. Target specific antibody carries typically cytotoxic compound to the target tissue. (Shastry et al., 2023). When conjugated with other molecules, DARPins can also act as carriers. In that case, DARPin just need to have a binding property, and the conjugate is functional molecule. The approach requires lower concentration of effective molecules and allows utilizing molecules with otherwise narrow or non-existent therapeutic window; in other words, when toxic dose of free molecule approaches or exceeds the effective dose. (Zhang et al., 2022).

Functional DARPin drug conjugates have been construed and researched. One of them (Karsten et al., 2022) targets EGFR and has MMAE, a cytotoxic short peptide, as a payload. To conjugate MMAE into DARPin, strain-promoted azide-alkyne cycloaddition (SPAAC) reaction was utilized with DBCO containing linker and azide-labeled DARPin. MMAE is a common compound used in ADCs. It acts by preventing microtubule formation, leading into cell apoptosis (Best et al., 2021).

1.3.4 Radio DARPins

In radio-DARPins, the effective conjugate is a radioactive compound and DARPin is binding into tumor-specific target for example. Radioactive compounds conjugated to antibodies are demonstrated previously. (Lizak et al., 2023)

Advancements in preclinical studies have been achieved with radio-DARPin. MP0712 is DLL3 targeting DARPin from Molecular Partners. DLL3 is overexpressed in many cancers, especially lung cancer (Owen et al., 2019). MP0712 has a radioactive lead isotope ^{212}Pb as payload. (Orano Med, 2024)

1.3.5 Multispecific DARPins and switch platform

When different DARPins are linked together, the product can bind to multiple epitopes, making the binding bi- or multivalent and thus stronger. When targeting pathogens with fast changing surface proteins such as RNA viruses, or tumor targets, having multiple DARPins also protects the binding capabilities against individual mutations. Bispecific antibodies have already been approved for clinical use, most often activating immune cells as cancer treatment (Esfandiari et al., 2022). Similar mechanisms of action can be achieved with DARPins linked together.

With recently patented method, is possible to construct a DARPin combination that binds to two different targets while the binding is mutually exclusive. That enables activating and inactivating the DARPin based on the presence of specific sensor target, creating switch-DARPin. Binding of sensor target prevents the therapeutic DARPin from binding to its target. Multispecific DARPin can also activate in presence of sensor target, that requires interaction between three DARPins. In initial configuration, DARPin in the middle binds to the therapeutic DARPin, preventing the binding to therapeutic target. Second DARPin and sensor-DARPin have mutually exclusive binding properties.

Binding of sensor target activates therapeutic DARPin by preventing second DARPin inhibiting it. The approach is useful if the therapeutic target is equally present in healthy tissue. For example, therapeutic DARPin could be functional only in certain tumour microenvironment, targeting proteins that would cause serve side effects if targeted without tissue-specific method. (FONTAINE et al., 2023). Similar approaches have been utilized with antibody based therapies (Kamata-Sakurai et al., 2021).

1.3.6 Car-T cell therapy

CAR-T cell (Chimeric Antigen Receptor T cell) therapy is clinically used treatment against cancer (Mullard, 2022). The cells naturally act as part of human immune system identifying antigens with the surface antibodies. T-cells can release cytotoxins to kill the recognized targets or release cytokines to activate other parts of the immune system. For therapy, CAR-T cells are extracted from a patient and genetically engineered to express the selected antibody. When injected back to patients, modified CAR-T-cells identify and neutralize the intended target based on the antibody binding. (Johnson & June, 2016)

Human immunoglobulin derived scFvs are mostly used as binder proteins. Other scaffolds have been utilized such as nanobodies, to improve the stability of binding proteins. DARPins have been researched for that purpose as well. Similar performance compared to other technologies has been obtained. (Nix & Wiita, 2024). On top of tumour targets, DARPin based CAR-T cell therapy could be used to eliminate HIV (human immunodeficiency virus) possessing cells. (Patasic et al., 2020).

1.3.7 DARPin therapeutics in clinical trials

Despite extensive research, there are currently no DARPin based therapeutics in the market. Researchers from University of Zurich have founded Switzerland-based company Molecular Partners (SWX:MOLN) that focuses on commercializing the DARPin technology. A few DARPin therapeutics have advanced to clinical testing, all developed by or in partnership with Molecular Partners.

Previously, one therapeutics was not approved after phase 3 trial due to its side effects. Abicipar, MP0112 is a single domain DARPin. It was developed as a treatment for neovascular age-related macular degeneration, a common retinal disease among elderly people, causing vision loss. It targets anti–vascular endothelial growth factor and is

administered by sequential intravitreal injections. Compared to antibody fragment based ranibizumab, similar therapeutic effect was achieved with lower injection frequency. The issue was higher incidence of intraocular inflammation (>15 %) during the first 52 weeks compared to ranibizumab (0.3 %). During the later 52 weeks, the inflammation was in similar level for both. The reason for inflammation was unclear but it was speculated to be caused by impurities from *E. coli* production. After optimizing the production conditions, incidence of inflammation was reduced to 8.9% among the group. (Allergan, 2020; Khurana et al., 2021)

MP0250 (Figure 3) is a trispesific DARPin inhibiting vascular endothelial growth factor (VEGF) and hepatocyte growth factor receptor (HGF). Both targets have significant role in development of multiple myeloma (MM). Inhibiting both targets simultaneously reduces the risk of cancer becoming resistant to the treatment. Clinical evaluation of MP0250 discontinued after phase 1b due to the lack of evidence on antitumor activity and due to existence of alternative treatments. The trial was executed with 33 patients relapsed / refractory multiple myeloma (RRMM), meaning the disease has returned after treatment or does not respond to a treatment. The patients were simultaneously injected with bortezomib/dexamethasone which is a typical treatment for MM. While the overall response rate (patients with partial recovery or better, ⩾50% reduction in biomarkers, Durie et al., 2006) was 32 %, it is challenging to separate effects of different drugs. The trial lacked a group with only MP0250 treatment, also control group without MP0250 treatment. (Baird et al., 2021; Binz et al., 2017; Knop et al., 2024)

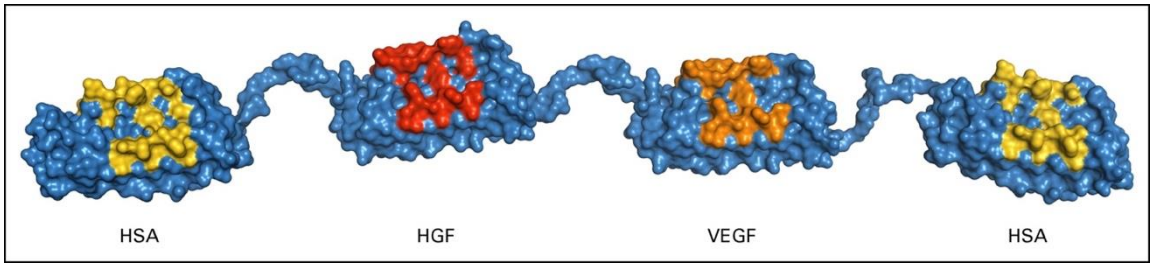

Figure 3. Protein structure of MP0250 drug candidate, similar structure is shared among other multispecific drug candidates from Molecular Partners. DARPins are linked together with polypeptide linkers. Therapeutic target specific domains (HGF and VEGF) are located in the middle. Human serum albumin (HSA) binding domains are in the edges to improve pharmacokinetic properties such as half-life in serum. (From Binz et al., 2017)

MP0274 is HER2 (human epidermal growth factor receptor 2) targeting drug candidate. While it is expressed in low levels in healthy tissue, in roughly 20 % of breast cancers overexpress HER2, especially advanced ones. Overexpression in cancer increases cell division and limits apoptosis. MP0274 has specificity to two different epitopes in HER2

increasing its binding capacity, which supresses cell growth or induces apoptosis in cells. In a case study with a 37-year-old female patient with metastatic HER2 positive breast cancer, 13 cycles of MP0274 treatment over a half year period lead to 78% tumor reduction. In total 22 patients were tested with different dosages in phase 1. The woman presented in case study was the only patient with the highest dosage (12 mg/kg) and the only one with significant response to the treatment. no severe side effects were observed meaning maximum tolerated dose was not reached. (Fiedler et al., 2017; Fischer et al., 2022)

MP0317 is a multi-specific switch-DARPin for solid tumors, targeting fibroblast activation protein (FAP) and CD40. CD40 is a transmembrane protein that activates immune cells. Normally, targeting CD40 causes severe side effects by nonspecific activation. In contrast, MP0317 is active only in presence of FAP, target overexpressed by cancer-associated fibroblasts. That enables targeting CD40 only in specific tumor microenvironment, reducing side effects by peripheric CD40 activation. The safety was proven in phase I clinical trial with different doses, as well as sufficient efficiency to forward in clinical testing. (Gomez-Roca et al., 2024; Ioannou et al., 2021; N et al., 2022; Steeghs et al., 2024)

MP0310 is a immune cell activating bispecific DARPin drug candidate for solid tumors. General issue with immune cell targeting binders have been side effects caused by immune cell activation outside of tumour microenvironment. MP0310 binds to 4-1BB (CD137) on T-cell. T-cells are activated when enough 4-1BB are clustered on its surface. That only happens in presence of FAP overexpressed by cancer cells, that other domain of MP0310 binds to. (M. T. Stumpp et al., 2020). Phase 1 was completed in 2022 (Molecular Partners AG, 2022). In press release (Molecular Partners, 2022) Molecular Partners indicated positive results from phase 1 that support further studies, but the data is not published.

Ensovibep (MP0420) is a potential treatment against Covid19. Angiotensin-converting enzyme 2 (ACE2) is a surface protein that the enables Covid19 entering the host cell. Trispesific DARPin binds to the receptor with all the domains preventing the interactions. Trispecificity prevent the virus becoming resistant by a single mutation. MP0420 demonstrated strong performance in preclinical studies, both in vitro and in vivo dwarf hamster model, independent of virus variant. (M. Stumpp, 2021). The clinical trials

advanced to phase 2 with 485 hospitalized covid patients. However, as a conclusion, ensovibep did not improve patient recovery (ACTIV-3/TICO Study Group, 2022). Molecular Partners has also MP0423 with similar structure and mechanism of action. (Rothenberger et al., 2021)

MP0533 is tetraspecific T-cell engager against acute myeloid leukemia (AML). One domain binds to T-cells activating CD3 protein while three domains target AML specific targets CD33, CD123 and CD70. As avidity to all three targets is higher than to individual protein, cytotoxicity to healthy cells which express only one antigen is supposed to be low. First in human clinical data with 37 participants was published recently. As adverse events 24 patients 65% had cytokine release syndrome (CRS) but out of those, only 3 incidents were grade 3, severe or medically significant. Infusion-related reactions were also common, with 21 events, 4 incidences were grade 3. 50% of patients showed reduction in bone marrow blasts, white blood cells related to leukemia. The data was encouraging to continue clinical testing. (Jongen-Lavrencic et al., 2024).

1.4 Display methods

1.4.1 Purpose and general concept

To enable binder selection from the library, display technologies are utilized. The idea is to have the binder library in protein-form while it is physically connected the translated protein's DNA or RNA sequence. DARPins interact with the with the target only as proteins, and amplification or almost any additional work with binders requires access the DNA of the protein. Cell-free display methods such as ribosome, mRNA, and DNA-display utilize in vitro translation and reverse transcription produce complex containing protein and RNA or DNA. In phage, and other cell-based methods, proteins are translated by the cells and expressed as surface proteins.

In cell free methods and in phage display, binders are selected from the library by biopanning. The displayed library is presented to the target that is typically immobilized to some surface. The surface is washed, and the remaining binders are collected. Due to really small binder - non-binder ratio in the initial library, the panning is repeated usually multiple times with amplified outputs. In cell-based displays, amplification is done by growing the cells and for phage, by multiplying them in the host cells. For cell free-displays, RNA is reverse transcribed if necessary and DNA is amplified by PCR. Cell

free methods are generally capable of handling libraries with 10^{12}-10^{14} binders, while cell-based systems are usually limited to 10^{8} molecules. Phage display functions with diversity up to 10^{11}. (Park & Cochran, 2010)

1.4.2 Cell-free methods

Ribosome display has widely been used for DARPin libraries. Compared to other display methods, ribosome display enables using largest libraries. The method relies on complex of RNA, ribosome and expressed protein. DNA is transcribed into RNA and translated in vitro. RNA sequence after the expressed protein prevents ribosome detaching from RNA. As stop codon is not reached, protein stays in the complex. The complex is held together only by non-covalent bonds. That makes ribosome display sensitive to harsh panning conditions. (Hanes & Plückthun, 1997; Park & Cochran, 2010).

Like ribosome display, the concept of mRNA display is similar. Instead of protein-ribosome-RNA complex, expressed protein is covalently connected to mRNA via puromycin linker. The link is relatively stable, and lack of ribosome reduces unwanted interactions with the target. Both ribosome and mRNA display are sensitive to RNA degradation due to poor stability of RNA and commonness of RNase as contaminant. The biopanning is typically carried out in ambient temperature for that reason. (Park & Cochran, 2010).

In DNA-display, mRNA is reverse transcribed into cDNA after translation and covalently linked to the protein. That creates a robust complex that can be used in various panning conditions. Linking the cDNA to the protein is not trivial. While many different methods exist (Kurz et al., 2001; Tabuchi et al., 2001), challenges in creation of protein-DNA complex has limited wider adaptation of the display method.

Recent advancements in linking have enabled one pot reaction from DNA to protein-cDNA complex with commercially available reagents. Transcribed mRNA is crosslinked to puromycin-containing oligonucleotide linker. Protein is translated and linked to puromycin. RNA is reverse transcribed using the oligo linker as primer. Transcription, crosslinking, *in vitro* translation, and reverse transcription reactions are carried out sequentially in approximately two hours. (Zeng et al., 2023).

DNA display with simple protocol and short generation time would combine the speed, accuracy and capacity of RNA display with robustness of phage display. Free selection

of panning conditions does not limit the type of targets. That would make DNA display an attractive method and allow wider adoption of it.

1.4.3 Phage display

Phage display offers a robust and stabile display platform While the size of the library is more limited compared to cell free methods, it is still significantly higher compared to other cell-based display methods. Display with M13 filamentous bacteriophage is widely used with antibody libraries while secretion (Sec) pathway is utilized. Proteins need to be in unfolded form in E. coli cytoplasm. That naturally occurs with antibodies, but the fast folding of DARPins is causes low display level. Using signal recognition particle (SRP) instead, enables protein translocation towards periplasm while still being translated. (Steiner et al., 2008).

For display, DARPins are cloned into phagemid vector. When *E. coli* is transformed with the vector and transfected with helper phage, the cells produce phage that are expressing individual DARPins as their P3 surface proteins. After selection round, phage can be amplified in the same *E. coli* strain.

1.4.4 Cell surface display

By linking the displayed protein to one of the surface or transmembrane proteins of the cell, many different hosts can be used as display platforms. Fluorescence-activated cell sorting (FACS) is generally used for selection. In that case, the target is tagged with fluorescence label, and the complex is freely binding to the cells expressing binder. Assuming similar expression level among cells, bound fluorescent labelled target is relative to the affinity of the expressed binder. Dedicated device for flow cytometry measures fluorescence from each cell and sorts the cells according to given parameters. When calibrated, cell sorting enables extracting cells and binders with desired affinities. High-throughput devices are capable of handling up to 10^9 cells. To get more accurate information about affinity related to display levels, it is possible to normalize target binding by the display level. In dual-color FACS, target and displayed protein are labelled with different labels. Display level and affinity can be considered separately and binder expressing cells selected based on both parameters. (Park & Cochran, 2010).

Prokaryotic, bacterial display, such as *E. coli* is the simplest example of cell surface display. Simple production and easy genetical modifications are the main advantages. Due to simple translation system, expressing more complex proteins can be a challenge. With DARPins, that should not be an issue due to their easy foldability and lack of need for post translational modifications. Large library can be preselected with magnetic cell sorting (MACS) before FACS (Song et al., 2019).

Yeast being eukaryotic organism has capability of displaying more challenging proteins, also to perform most post-translational modifications. Up to 10^9 cfu libraries have been reported with yeast display, but typically 10^6-10^7 cfu is more achievable (Könning & Kolmar, 2018; Park & Cochran, 2010). Yeast display can be combined with higher throughput selection methods to narrow down the initial library and therefore increase the display capacity (Schütz et al., 2016).

Mammalian display is usually done in CHO (Chinese Hamster Ovary) cells or HEK (Human Embryo Kidney) cells. On mammalian cell surface, a complex protein is the closest to its natural form, especially if meant to be produced in mammalian host such as antibodies. Other advantage in using eukaryotic or mammalian display is higher display capacity in an individual cell. As a result, affinity estimate is more precise during cell sorting. (Park & Cochran, 2010; Zhou et al., 2010).

1.5 DARPin library

The DARPin library used in the experiment (referred as R0 in experimental part) has been developed in Turku University by PhD Tuomas Huovinen et al. DARPins in the library (Fig 4) have variable amino acids in second diversity motif, D2. With six amino acids fully randomized, the library has theoretical diversity of 2.4 $x10^{11}$. The design allows affinity maturation after the first selection rounds by randomizing variable regions also on D1 and C-cap.

DARPin DNA had been cloned into VCM M13 phagemid vector to enable phage display. The signal sequence was optimized, leading into improved display efficiency (Kulmala et al., 2022). Having the theoretical diversity limited by only one motif of DARPin fully randomized, enables achieving better coverage of the library with phage display.

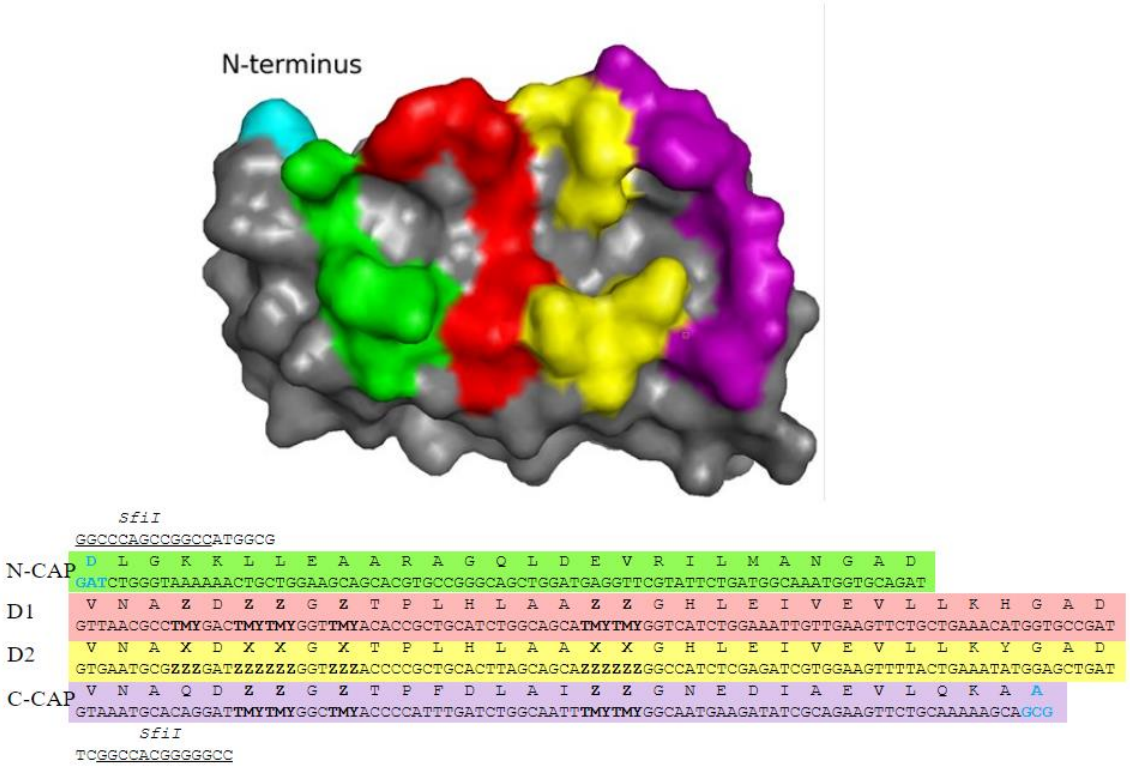

Figure 4. 3D structure of DARPin and the corresponding DNA sequence. Variable locations (**ZZZ**) in D2-repeat contain randomized amino acids excluding proline and cysteine. Variable locations in D1 and C-cap (**TMY**) contain degenerate mix of tyrosine and serine. Unidentical corresponding codons in D1 and D2 enable repeat specific DNA modifications.

1.6 Aims of the study

The library from University of Turku had previously been tested against a few well-known proteins with positive outcome (not published data). In this study, clinically relevant targets were used. The library was screened with phage display against two undisclosed target proteins, X and Y in collaboration with the Biologicals unit of Orion Pharma. In parallel, glutathione-S-transferase (GST) was used as a positive control protein for selections. GST is generally used as a protein tag.

From panning outputs, binders against X and Y were validated and characterized without additional maturation steps. Multiple binders against both targets with high affinity and wide epitope coverage was a desired outcome. That means that DARPins need to bind to different locations in the target.

In antibody related work, the compound that antibody binds is usually referred as antigen. The term is shortened from “antibody generator”. For clarity, in this work, proteins that

DARPins are selected against are generally referred as targets, the term used more frequently in drug development context.

2 Materials and Methods

2.1 Biopanning

Neutravidin coated beads were produced using Dynabeads™ Antibody Coupling Kit (Thermo Fisher) and 25 µg neutravidin per 1 mg of beads. The beads were diluted to concentration of 10 mg/ml. Bead capacity was tested using excess (=0,2*1,25 µg/5*10 µg) biotinylated EU-labelled BSA. Fluorescence signal was compared to M280 dynabeads and to an old batch of neutravidin coated beads.

4 ml R0 phage stock at $5*10^{12}$ cfu/ml was diluted 1:4 with TBS and precipitated using 1/5 v/v PEG-NaCl on ice for 60 min. After spinning 20000 rcf for 10 minutes the precipitate was dissolved in 1 ml TBS. Phage titers were determined by oligonucleotide-directed chelate complementation assay OCCA (Lehmusvuori et al., 2012) or by qPCR.

Details for each panning round are shown in Table 1. Following general protocol was used for biopanning with beads:

The beads were prewashed 2 x with 1 ml TBT-0.05 (TBS + 0.05 % w/v Tween) and once with 1 ml TBS. Beads were incubated in rotation with biotinylated target at 0.5 ml in target specific buffer 0,5 h at room temperature. Target coated beads were washed 3x with panning buffer. Phage binding was done at 1 ml RT in rotation for 1h. Beads were washed 3x and the tubes were changed after 1st and 3rd wash. Phages were eluted from beads with 60 µg/ml trypsin in 100 µl 30 min reaction RT. Phages were infected into 1 ml log-phase (OD600 0.2-0.7) XL1-b cells by 60 min incubation at 37 C, followed by plating to GTC plates.

For phage production, the overnight growth from plates was harvested and inoculated to SB medium with 50 µg/ml tetracycline and 50 µg/ml chloramphenicol at OD 0.05. When reaching a log phase at 37 C, around 20 MOI VMC M13 helper phage was added. In practice, 0.5 µl helper phage stock was added for 1 ml cell culture. After additional 60 min incubation, 30 ug/ml kanamycin was added followed by an overnight incubation at 30 C. The culture was centrifuged 4000 rcf 10 min and phage were precipitated from the supernatant using 1/5 v/v PEG-NaCl on ice for 60 min. After spinning 20000 rcf for 10 minutes, the precipitate was dissolved in 1 ml TBS. The phage stock was used for next panning round or for phage immunoassay.

The first attempt of round one is marked as PN in table 2. Dr. Tuomas Huovinen repeated the panning. That output (TH) was used in second round. The third round was done as panning in solution. Instead of immobilized target, the phages were incubated in low concentration of biotinylated target for 1 h. The phage-target complexes were rapidly captured in 5 min incubation with streptavidin beads. In fourth panning, the aim was to lower the number of nonspecific binders by extending the washing step. Antigen was immobilized in streptavidin plate. The unbound material was washed four times with plate washer using Kaivogen washing buffer. After phage binding, the plate was washed 16 times. Each reaction was done in three parallel wells that were combined after elution. At the same time, the fourth panning round was conducted using beads and standard protocol.

Table 2. Panning details.

Round	Target and condition	Target immobilization or capture	Bead, µl (10 µg/µl)	Biotinylated target	Phage input, µl/CFU	Phage production after panning round, ml
R1 PN	X, Y, XT[a], YT, GST	M280 Streptavidin	20	Saturated (1 µg)	400/ 4e12	-
R1 TH	X, Y, XT, YT, GST	MyOne STR C1	20	Saturated (8 µg)	500 / 5e12[b]	20
R2	X, Y, XT, YT, GST	Neutravidin	10	Saturated (1 µg)	20 / 2e11 [c]	5
R3	XT, YT, GST	M280 Streptavidin	10	1 nM (in solution)	1 / 1e10	5
R3[d]	X, Y	M280 Streptavidin	10	1 nM (in solution)	4 / 4e10	5
R4-1	X, Y, XT, YT	Streptavidin plate	-	50 ng /well	1 / 1e10	5
R4-2	X, Y, XT, YT	M280 Streptavidin	10	Saturated (2 µg)	1/ 1e10	5
R5[e]	Y	M280 Streptavidin	5	1 nM (in solution)	5 / 5e10	5

a. T: with Tween-20, containing 0.05 % w/v Tween in the binding and 0.1 % w/v in washing buffer.
b. For R1 TH, the deep freezed phage stock was not precipitated for glycerol removal.
c. Phage titer for later rounds was assumed phage stock titer obtained by standard protocol (1E13 cfu/ml)
d. Round three was repeated for Tween-free reactions with R2 stock with higher phage input.
e. Combination library from Y-DARPins by off-rate and in-solution panning. Phage production volume represents amplification of the library before the panning.

For screening, the colonies were picked into 96-plate containin g 160 ul LB medium with tetracycline, chloramphenicol and 0.5 % glucose. From O/N culture, 2 µl growth was taken into phage production plate containing LB, T and C. After 5 hours of incubation, 20 MOI helper phage was added and incubated O/N. Cells were centrifuged and 2 µl supernatant was used in phage immunoassay.

2.2 Phage immunoassay

Phage immunoassays were performed in streptavidin coated clear well-plate (Kaivogen). The plate was saturated with 50 ng target protein incubated in 100 µl Kaivogen assay buffer at RT low shaking for 30 min. Wells were washed 4x. Phage sample was incubated in 1 h in 100 µl of assay buffer, followed by 4 x plate wash. 50 ng N1-EU anti-VMC-M13 antibody was incubated for 45 min before washing the plate 4x. 200 µl DELFIA enhancement solution was added, and the plate was incubated 10 min in shaking before measurement with Victor 1420 Multilabel Counter.

For binder enrichment measurement, PEG-NaCl purified phage stock from each panning round was used in triplicate, targeting 1e7 phage per well. For colony screening, 2 µl of supernatant from phage production plate was used without dilution. As background, wells with phage and without target were used.

2.3 DARPin combination library

DNA was extracted from XL1 5 ml overnight culture. Mix of Y and YT from round four was amplified, and linkers were added by primers (PCR 1 in table 3) in 8 parallel reactions. The product was purified with PCR purification kit. After BspQI digestion and gel extraction, samples were ligated combinatorially using T4 ligase. The product (6 parallel samples) was gel extracted and amplified (PCR 2). PCR purification and SfiI digestion were followed by BspQI digestion. The product was gel extracted but the relative amount of correct size product was low in the gel. Gel-ex product was amplified again with higher annealing temperature. After SfiI and BspQI digestion, DNA was gel extracted and ligated with pEB3v3a vector.

XL1b cells were transformed using 2 µl of ligation product directly (from total 100 µl) in 80 µl electrophoresis reaction (Bio-Rad Genepulser 1.25 kV, 25 µF, 200 Ω). Rest of the

ligation product was concentrated with Zymo purification kit to 6 µl. Electrophoresis was repeated with 2 µl of the concentrated product. The cells were recovered with 1 ml SOC medium and incubated 60 min at 37 C and 300 rpm, followed by phage production.

Table 3. PCR reactions for combination library creation

N:o	Template	Forward primer	Reverse primer	Linker between DARPins	Annealing
1	R4 output, DNA miniprep from XL1 culture	TH348 TH348 TH348 TH348 JT0013 JT0014 JT0015 JT0016	JT001 JT002 JT003 JT004 TH347 TH347 TH347 TH347		60 °C
2	Ligated ARD-ARD	TH348	TH347	1:GGGS 2:GGGGSGGGGS 3:GGGGSGGGSGGGGS 4:GGGGSGGGGSGGGSGGGGS 5:GGGGSGGGGSGGGSGGGGS GGGGS 6:GGGGSGGGGSGGGSGGGGS GGGGS-GGGGS	60 °C
3	Amplified ARD-ARD	TH348	TH347	As PCR 2	65 °C

Binder selection from combination library (5th round) was performed as off rate panning. The panning followed the principle of round 3 except after phage binding, unbiotinylated target was added in the reaction to compete with biotinylated target for 30 min. In parallel, one reaction was conducted with only the biotinylated target.

2.4 Sequencing

A plate of each X- and Y-binders were sequenced at Eurofins genetics. Liquid culture samples were sent on Eurofins Colony Sequencing Plate. M13rev-29 Standard Primer was used.

The sequences were initially analyzed using Biopython package. DARPin amino acid sequence was extracted and saved in a .csv file with the following python commands:

```
import csv
from Bio import SeqIO
from Bio.Seq import Seq
with open("path_of_a_precreated_csv_file", 'w', newline='') as csvfile:
   seqwriter = csv.writer(csvfile, delimiter=' ', quotechar='|',
quoting=csv.QUOTE_MINIMAL)
   for record in SeqIO.parse("path_of_the_fasta_file", "fasta"):
      seqwriter.writerow([   record.description[-3:],
Seq(record.seq[record.seq.find('GATCTGGGTAAAAAA'):])[0:1000],
Seq(record.seq[record.seq.find('GATCTGGGTAAAAAA'):]).translate()[0:350]])
```

The csv file was analyzed in Microsoft Excel, comparing the variable region of DARPins and looking for enriched amino acid sequences.

2.5 Production construct

Production vector pOri 966 contained His-tag in N-terminus of the produced protein. Two methods were used to clone DARPins from pEB3v3a into pOri 966. The traditional restriction digest method relied on complementary sticky ends in the fragments created by restriction enzymes. NEB High Fidelity Assembly kit has the same principle as Gibson assembly, complementary overhangs are aligned during assembly.

In restriction enzyme-based approach, DARPins were amplified from XL1- pEB3v3a liquid culture with PCR (Table 4) and F1 and R4. PCR product was purified with NucleoSpin Gel and PCR Clean-up kit (MACHEREY-NAGEL), digested with restriction enzymes BamHI and Kpnl (NEB) and purified again with the kit. POri 966 plasmid backbone was produced in DH5α (NEB) and purified using NucleoBond Xtra Midi EF (MACHEREY-NAGEL). After BamHI / Kpnl digestion, vector was gel-extracted using 0.8 % agarose gel and NucleoSpin Gel and PCR Clean-up kit. The insert was ligated into vector in 50 µl reaction using T4 ligase and 1:3 vector-insert ratio.

NEB High Fidelity Assembly kit was used according to kit instructions. Vector backbone was amplified in PCR with R18 and F19. Insert DARPins were amplified from XL1-pEB3v3a using primers F6 and R8. PCR products were purified with NucleoSpin kit. Assembly time with NEB High Fidelity kit was extended to 60 min.

For heat-shock transformation, 2 µl T4 ligation product or 0.5 µl Gibson assembly product was added to 12.5 µl DH5α cells and incubated on ice 30 min. Heat shock was 30 seconds at 42 C, followed by 2 min incubation on ice. Cells were recovered in 250 µl

SOC medium and incubated at 37 C 800 rpm for 90 min. 125 µl of cells were spread on LB kanamycin (K) plates. After O/N at 37 C (alternatively over weekend at 22 C), single colonies were spread into plates. DNA from single colony from secondary plate was produced in 5 ml overnight culture. The success of the cloning was analyzed by PCR using intra-DARPin primers F11 R12. DNA was extracted from positive cultures with Miniprep (Qiagen).

Table 4. General PCR conditions used in DARPin amplification for production.

Step	Temperature	Time
Hot start	95 °C	Manual
Initial denaturation	98 °C	0:30
Denaturation	98 °C	0:10
Annealing	60 °C	0:20
Extension	72 °C	0:30
	Steps 3-5 repeated 30 times	
Final extension	72 °C	2:00
Hold	10 °C	Manual

2.6 Production and purification

0.5 µl vector was transformed into NiCo (NEB) production strain. Multiple colonies from O/N plate were transferred to 5 ml LB-K preculture. 4 x 125 µl preculture was inoculated into 4x 2500 µl TB-K on 24-well pate and grown at 37 C for 2 hours. Temperature was lowered to 18 C and IPTG was added. After 18 h incubation at 250 rpm, cells were harvested by centrifuging at 3000 g 15 min 4 °C. If not lysed directly, the pellet was frozen using liquid nitrogen and stored at –80 °C.

For lysis, 4 x 25 µl lysozyme solution was added. The pellet was resuspended into 4x 250 µl lysis buffer and four pellets were collected. 10 µl DNase mix was added and incubated on ice for 5 min. Cell lysate was centrifuged twice 1 h at 20000 rcf and diluted into 5 ml IMAC buffer.

DARPins were extracted in one step purification using affinity chromatography with Äkta and Ni columns. The chromatography was run with IMAC buffer. Elution fractions were collected and concentrated with 5 ml centrifugal filter with 3 kDa cut-off. 1:1 buffer exchange to IMAC was performed to reduce imidazole concentration after elution. For gel imaging, 20 µl sample was incubated with 8 µl reducing buffer at 95 C for 3 min.

2.7 Affinity measurement

DARPins binding to target was measured with OctetRED96e using SA streptavidin sensors and 1x Octet buffer in PBS pH 7.4 with measurement protocol shown in Table 5.

Table 5. Octet measurement protocol

Data Name	Assay Time	Reagent	Flow Rate
Sensor Check	30	Buffer	1000
Loading	600	100 nM biotinylated target	1000
Baseline	120	Buffer	1000
Association	600	DARPin	1000
Dissociation	600	Buffer	1000

Data was analyzed in Octet® Analysis Studio using global fitting and 1:1 model.

2.8 Epitope binning

A competitive sandwich assay was created for epitope binning. DARPins were buffer exchanged into PBS. DARPin was immobilized on 20 mM EDC and 10 mM NHS preconditioned AR2G sensor in 10 mM acetate pH 5 buffer. Target protein was let bind to immobilized DARPin. Last step was in premix of second DARPin and target, keeping target concentration constant.

2.9 List of reagents

Table 6.1. Reagents used

TBS	50 mM Tris-HCl at pH 7.5, 150 mM NaCl
PEG-NaCl	20 % w/v PEG8000, 2.5 M NaCl
Panning buffer X	1X TBS, 0.2mM DTT, 1 % BSA
Panning buffer XT	1X TBS, 0.2mM DTT, 1 % BSA, 0.05 % Tween (0.1 % Tween in washing)
Panning buffer Y	1X TBS, 0.2mM DTT, 1 % BSA, 2mM MgCl, 0.2 mM ATP
Panning buffer YT	1X TBS, 0.2mM DTT, 1 % BSA, 2mM MgCl, 0.2 mM ATP 0.05 % Tween (0.1 % Tween in washing)
Panning buffer GST	1X TBS, 1 % BSA, 0.05 % Tween (0.1 % Tween in washing)
SOC medium	0.5% Yeast Extract, 2% Tryptone, 10 mM NaCl, 2.5 mM KCl, 10 mM, MgCl2, 10 mM MgSO4, 20 mM Glucose, pH 7.5
LB medium	30 % tryptone. 20 % yeast extract 10 % MOPS, all w/v
GTC-plate	15 % agar, 0.5% glucose, 25 µg/ml chloramphenicol, 10 µg/ml tetracycline w/v

TB-medium	
Trypsin	60 ug/ml in TBS, diluted from stock (6 mg/ml in 1 mM HCl)
IMAC buffer	25 m MTris pH 8.0, 250 mM NaCl, 0.5 mM TCEP
IMAC elution	25 m MTris pH 8.0, 250 mM NaCl, 0.5 mM TCEP, 0.5 mM imidazole
Lysis buffer	5 mM Tris pH 8.0, 250 mM NaCl, 10 % glycerol, 0.2% DDM, 2mM TCEP
DNase mix	2.5 mg/l DNase I, 0.4 M MgCl, 0.01 M CaCl
Octet kinetics buffer	PBS + 0.1% BSA, 0.02% Tween-20 and 0.05% sodium azide
PBS	137 mM NaCl, 2.7 mM KCl, 10 mM Na_2HPO_4, 1.8 mM KH_2PO_4

Table 6.2. Primers

JT001	TATATAGCTCTTCCGCCACCACCCGCTGCTTTTTGCAGAACTT
JT002	TATATAGCTCTTCCACTGCCGCCACCACCCGCTGCTTTTTGCAGAACTT
JT003	TATATAGCTCTTCCACTGCCGCCACCACCACTGCCGCCACCACCCGCTGCTTTTTGCAGAACTT
JT004	TATATAGCTCTTCCACTGCCGCCACCACCACTGCCGCCACCACCACTGCCGCCACCACCCGCTGCTTTTTGCAGAACTT
JT0013	TATATAGCTCTTCTGGCGGCAGTGATCTGGGTAAAAAACTGCTG
JT0014	TATATAGCTCTTCCAGTGGTGGTGGCGGCAGTGATCTGGGTAAAAAACTGCTG
JT0015	TATATAGCTCTTCTAGTGGTGGTGGCGGCAGTGGTGGTGGCGGCAGTGATCTGGGTAAAAAACTGCTG
JT0016	TATATAGCTCTTCCAGTGGTGGTGGCGGCAGTGGTGGTGGCGGCAGTGGTGGTGGCGGCAGTGATCTGGGTAAAAAACTGCTG
P-Da F1	CACAGATCTGGTACCACCGGTAGCGATCTGGGTAAAAAACTGCTGGAAGCAGCACG
P-Da F4	TCAGTCGACTCATCAATTAAGCTTGGATCCGCCGGTCCCTCACGCTGCTTTTTGCAGAACTTCTGC
P-Da F6	ATGGGATCGCACCATCACCATCACCATCATCACAGATCTGGTACCACCGGTAGCGATCTGGGTAAAAAACTGCTGGAAGCAGCACG
P-Da F8	TAATTAACCTCGAGGCTCAGTCGACTCATCAATTAAGCTTGGATCCTTATCACGCTGCTTTTTGCAGAACTTCTGC

3 Results and Discussion

3.1 Biopanning and binder enrichment

During production, neutravidin beads unintentionally settled during overnight incubation as the rotator stopped. When compared to commercial streptavidin beads and previous batch of neutravidin beads, the batch of neutravidin beads showed less binding capacity compared to commercial streptavidin beads and previously coated neutravidin beads but biotin binding was on acceptable level (Figure 5).

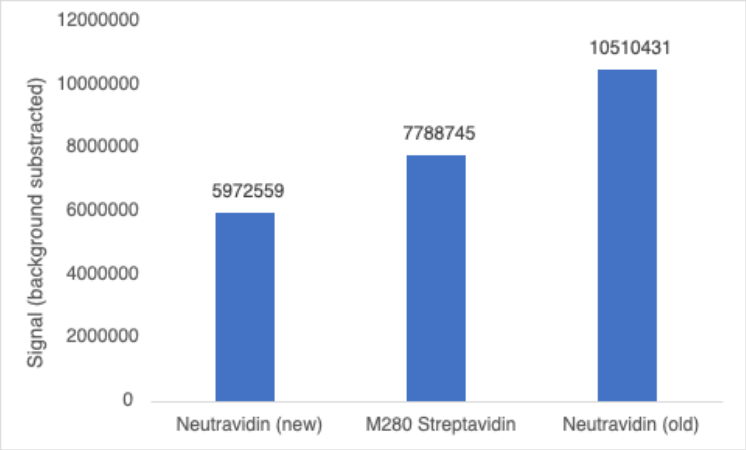

Figure 5. Biotinylated BSA binding capacity of different beads. Bead capacity was tested by binding an excess of biotinylated EU-labelled BSA on 5 µg of beads in triplicate. After washing the microbeads were incubated in enhancement solution and the solution was transferred on 96-well plate for time-resolved fluorescence measurement.

In panning, reactions with and without commonly used detergent Tween were performed against both X and Y. Target specific buffers were used preserve the target structure as well as possible. With that approach, lack of detergent caused the beads to scatter around the tube instead of pelleting normally in presence of a magnet. That resulted in visually noticeable loss of beads in washing and at the same time prolonged the time of that step. Both factors may have decreased the phage output. Including BSA in washing buffer seemed to improve the pelleting.

GST was chosen as a positive control because the binders could be further utilized as biotechnological tools, e.g., for pull-down experiments and as detection reagents in immunoassays and western blotting containing GST-tagged proteins. GST was panned only with Tween-TBS buffer.

Starting from the second round, background panning reactions without targets were performed. The outputs are shown in table 7 and figure 6. With almost all the targets, output-background ratio constantly increased over the panning rounds.

Table 7. Panning outputs calculated from dilution plates. With GST, only 3 panning rounds were performed. In sample names, + and – represent panning with and without antigen, respectively. R4.1 was performed with streptavidin plate and R4.2 with magnetic beads.

Round	X-	X+	XT-	XT+	Y-	Y+	YT-	YT+	GST-	GST+
R1	-	3.6E+07	-	7.2E+06	-	2.5E+07	-	1.0E+07	-	2.9E+06
R2	1.2E+05	2.8E+05	3.3E+04	5.2E+06	2.5E+05	1.2E+06	1.4E+05	2.8E+06	3.2E+04	5.5E+04
R3	4.7E+03	1.0E+06	1.0E+03	4.4E+04	1.8E+04	1.4E+06	1.0E+03	2.5E+05	5.0E+02	1.3E+04
R4.1	6.1E+04	1.2E+07	1.7E+04	4.1E+06	1.3E+05	9.2E+06	0.0E+00	4.4E+06	-	-
R4.2	6.1E+04	4.6E+06	1.7E+04	3.1E+06	1.3E+05	3.9E+06	6.9E+04	2.5E+06	-	-

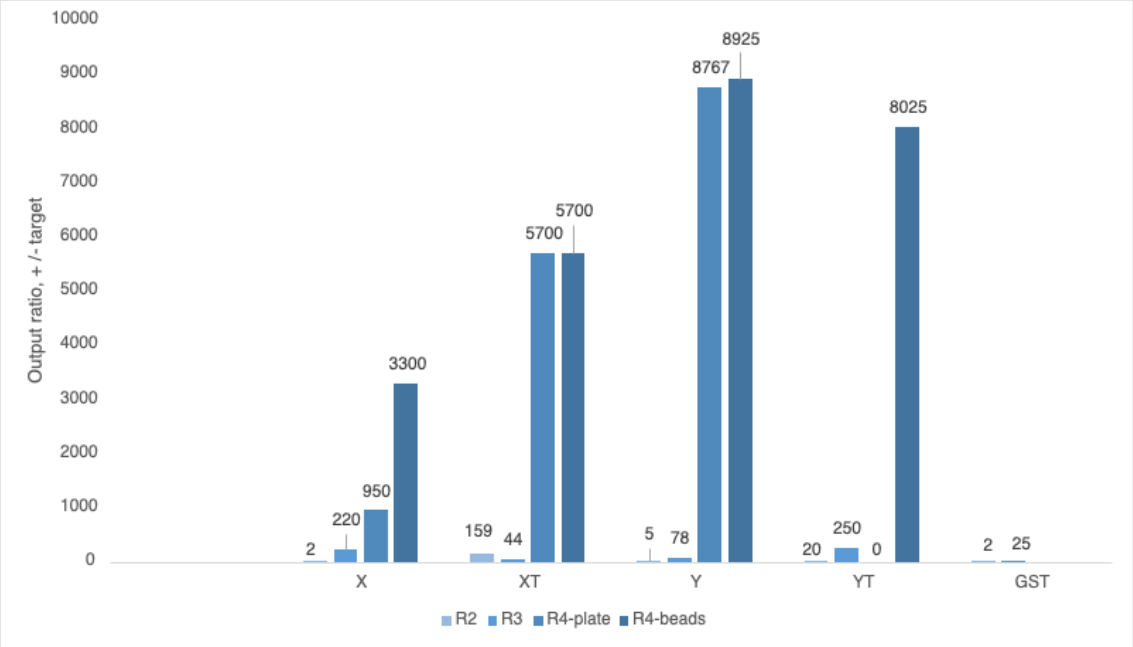

Figure 6. Positive panning / background ratios from of phage outputs. For YT R4 plate, the ratio could not be calculated as no colonies were formed in the background sample. The ratio indicates the portion of phage that bind to the target and not just to magnetic beads or tubes.

Binder enrichment was measured in phage immunoassay. The DARPin expressing phage were let bind to immobilized target protein. Phage binding was measured by adding europium labelled anti-phage antibody and measuring the signal. Enrichment from panning output represents polyclonal measurement. Colony screening on the other hand was performed with monoclonal samples. With monoclonal immunoassay, stronger DARPin binding to the target results in higher signal. With polyclonal sample, high signal is a result of both strong binding and the large number of binders in the sample. Even if these qualities are not necessarily distinguishable from the result, polyclonal phage immunoassay gives an overview of binder enrichment after a biopanning round.

Based on the significant enrichment according to phage immunoassay (Figure 7), colony screening was already performed from the third panning round. One more panning was still performed and colony screening was repeated for fourth round and for the panning with combination library.

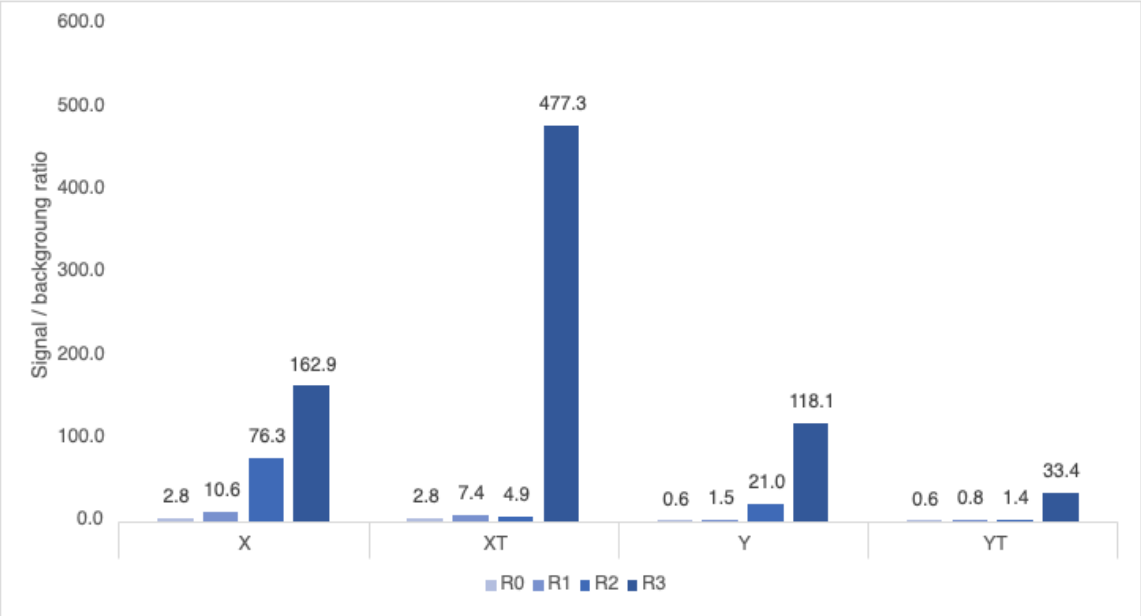

Figure 7. Binder enrichment in panning output based on polyclonal phage immunoassay over the first three panning rounds. R0 (the initial phage library) was once measured against each target.

3.2 Colony screening

Colonies were picked from dilution dishes to 96 well plates, phage were produced and screened with phage immunoassay. Unlike assumed from biopanning outputs, the hit rates (where S/B >3) from the third round were low for both X and Y. Percentages of binders from screened samples were 28 %, 43 %, 22 % and 3 % for X, XT, Y, and YT, respectively. In contrast, significant binder enrichment was achieved with GST already on round three, hit rate being 89 %.

Due to low output, bead-based panning and plate panning, rounds 4.1 and 4.2, were combined in colony screening. Hit rates for X, XT, Y, and YT were 61 %, 46 %, 26 %, and 5 %, respectively.

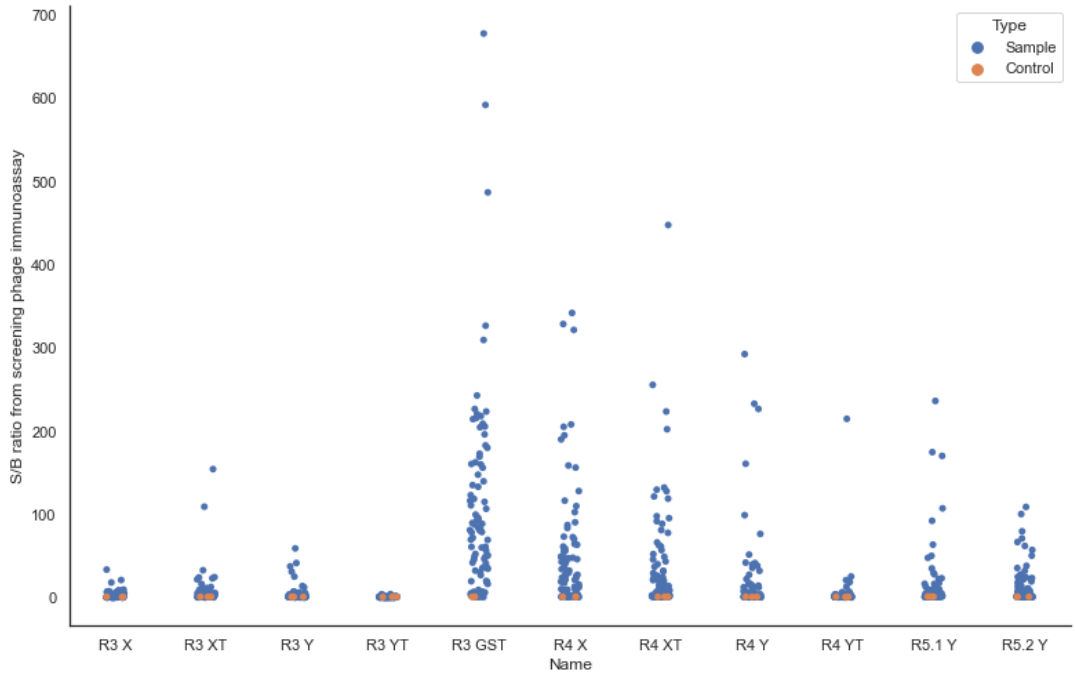

Figure 8 Signal-background ratios of colony screening samples from rounds 3, 4, and 5. R5.1 represent off-rate panning of combination library and R5.2 the corresponding in-solution panning.

3.3 DARPin combination library

As protein Y was considered more interesting target, the combination library was created from R4 Y and R4 YT outputs combined. The idea was to create stronger binders by bivalent binding Outputs were amplified with different linker-containing primers, ligated together to twin-DARPins and subcloned into pEB3v3a vector. Transformation into XL1 cells was successful (Figure 9). With background subtracted, over 50 000 insert-containing transformants were expected.

Outputs from both concentrated and direct transformation were used to produce phage stock used in round 5 panning. Phage outputs from R5 were relatively low (Figure 10). Still, compared to background (same background sample for both panning reactions), the outputs for off-rate and in-solution pannings were 52-fold and 350-fold. Lower output in off-rate panning was expected as competing unbiotinylated target was added to remove high off rate phage from biotinylated antigen.

Colony screening (Figure 8) from round 5 revealed that off-rate panning produced more high S/B binders compared to panning without competing antigen. Still, similar and even higher S/B ratios observed from round 4 individual Y-DARPins. As S/B ratios are not

always comparable and combination DARPins were not further characterized, accurate information of binding properties is not available.

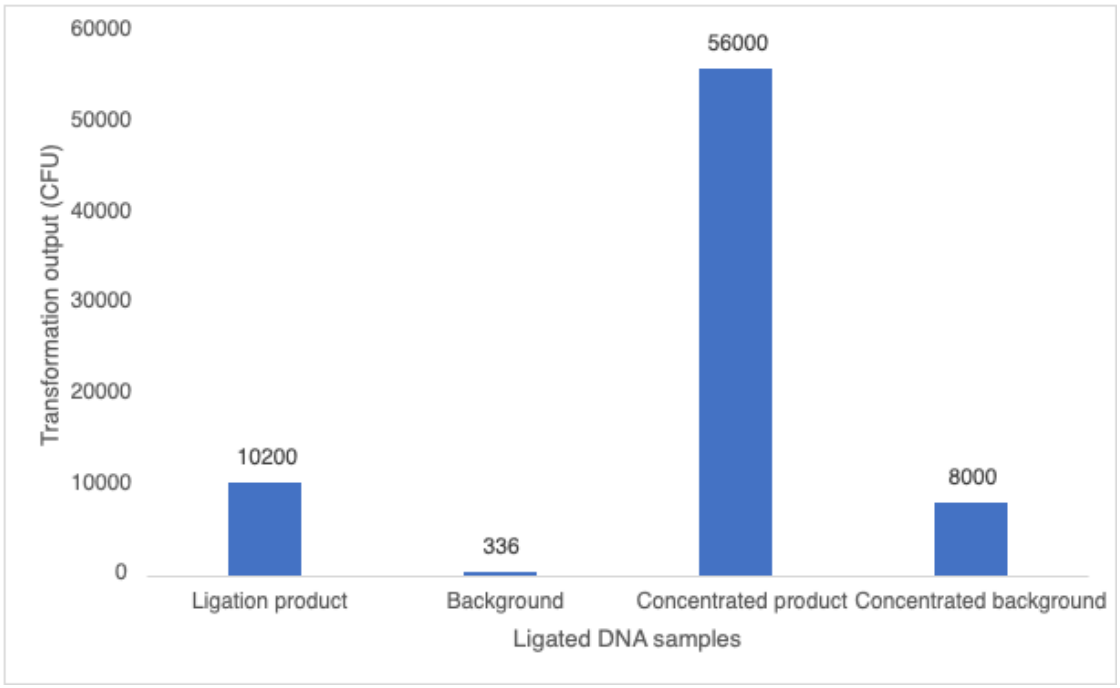

Figure 9. Electroporation of pEB3v3a-ARD-ARD product into XL1b cells. Ligation control without insert was used as background sample. With direct transformation and with concentrated product, backgrounds were 3 % and 14 %, respectively, compared to positive transformation.

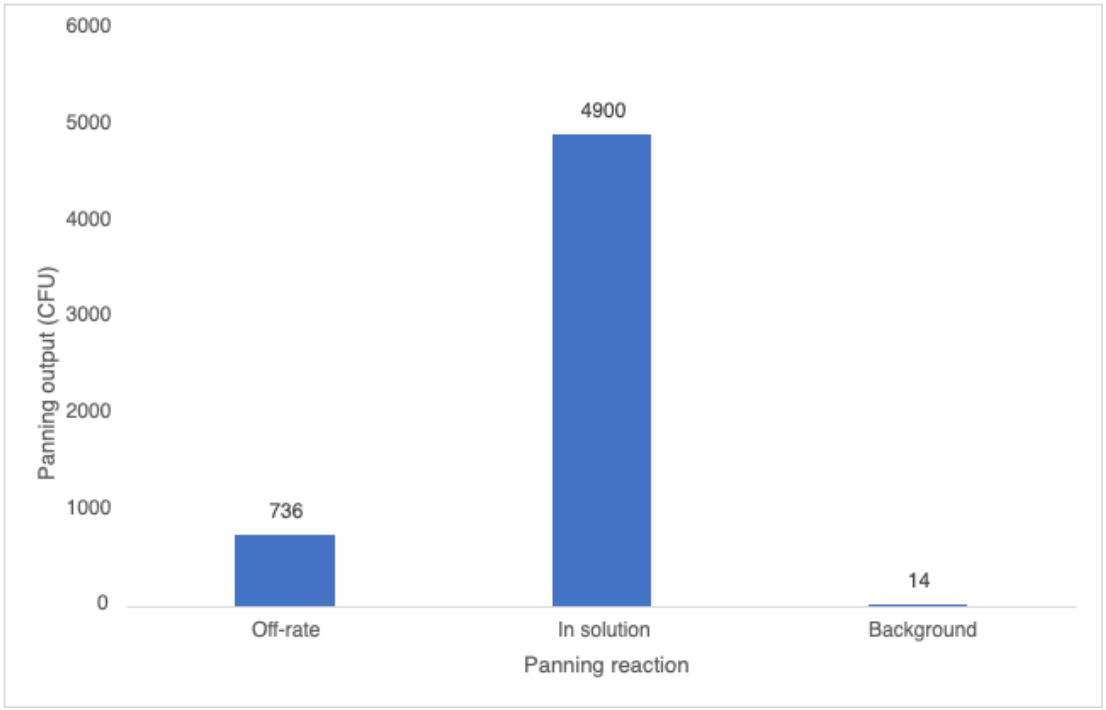

Figure 10. Panning output from round 5. In off-rate sample, competing unbiotinylated antigen was added after binding. Lower output is expected compared to in-solution sample with biotinylated antigen only. Binder enrichment phage immunoassay for was not performed for R5 samples.

3.4 Sequencing

X and Y - binders with the highest S/B ratios from colony screening phage immunoassays were picked from R4 to the fill two 96 sequencing plates, one for each target. Most of the sequenced DARPins were unique. Out of 84 successfully sequenced Y-DARPins, there were three pairs with the same sequence, (YH7, YF11), (YG7, YTA9), and (YTB6, YTC6). For X, number of successful sequences was 90 and 5 pairs had identical sequence, (XC2, XC3), (XD2, XD3), (XF5, XF6), (XG6, XG7) and (XH5, XH6). Low number of identical colonies in screening indicates relatively low overall binder enrichment. Identical clones in X-plate being adjacent rises a suspicion of cross-contamination during colony screening.

Looking at hydrophobicity of variable amino acids (Mozhaev et al., 1988), panning without tween produced more hydrophobic DARPins on average for Y but less hydrophobic for X (Table 8). For either group, the difference was not statistically significant. Based on the results, the presence of detergent does not significantly favour binding based on the binder's hydrophobicity.

Table 8. Average hydrophobicity of variable amino acids in sequenced DARPins. P-values for null hypothesis (X=XT, Y=YT) were calculated with average hydrophobicity of variable region in individual DARPins using two-sided Mann-Whitney U-test (Mann & Whitney, 1947; *Scipy/Scipy/Stats/_mannwhitneyu.Py at v1.14.1 · Scipy/Scipy*, n.d.)

X	XT	Y	YT
12.33	12.37	12.33	12.24
p-value=0.36		p-value=0.43	

3.5 Production construct

Both F1 R4 and F6 R9 PCR amplified DARPins successfully. Heat shock transformation with ligation product produced typically > 100 colonies in the selection plate. Clones were verified with PCR with intra-DARPin primers (Figure 11) Most of the clones by restriction digest method were positive but typically negative ones as well. With NEB HiFi assembly, significantly more clones were positive compared to restriction digest method.

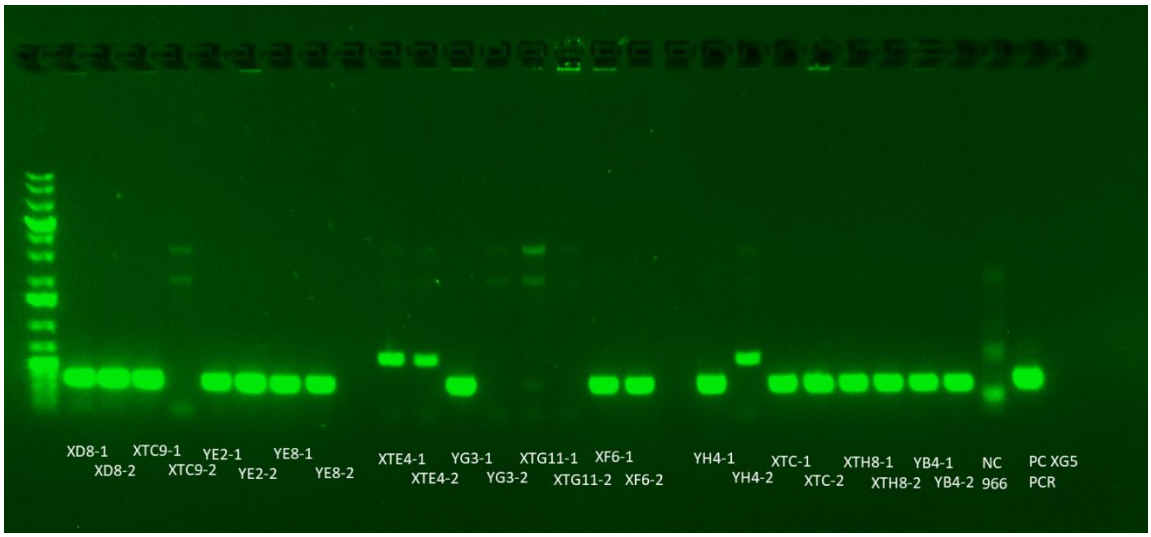

Figure 11. Electrophoresis of a F11, R12 PCR validation of a DARPin in the production vector cloned by restriction digest. F1, R4-amplified DARPin was used as positive control (last sample) and an empty vector as negative control. Samples with longer PCR product (XTE4-1, XTE4-2, YH4-2) were considered negative.

3.6 Production and purification

Both TB medium with IPTG induction and MagicMedia™ auto induction medium were used for production. Protein production was determined by UV absorbance at 280 nm with Nanodrop spectrometer. Production levels from 10 ml volume were generally low (Table 9), all below 0.2 g/l. One sample, YB5 resulted in negative protein concentration, which showcases the relative inaccuracy of the measurement in low concentrations.

Table 9. Yields from 10 ml production after purification and concentration. M in the name means production with auto induction medium.

Sample	Yield, µg	Sample	Yield, µg
YE2	22	XG5	1808
YD2	54	XE9M	156
YB4	23	XG5M	68
YC11	75	XD9	37
YE8	44	XA3	189
YH4	41	XC4	936
YB5	-33	XB11	727
YG3	54	XC4-2	48
YE10	101	XD9M	31
YG11	44	XC5	563
YE9	218	XC10	272

Based on SDS-page images (Figure 12), one-step purification was effective enough, most of the protein was DARPin. Only XB11 showed clear protein bands other than produced DARPin. It seems that samples with low measured protein concentrations (YB4, YE2) did not contain any protein. These samples were not further processed. Some of the flow-through samples were also run in the gel. Some FT samples were empty, especially YG11 and YH4 that in gel were located away from concentrated samples. Flow through samples loaded next to concentrated samples (XA3, XB11, XC4) showed a visible protein band. It is unclear whether protein was already in the flow through sample, or it was flown to the well from the nearest concentrated sample when loading the gel. In either situation, most of the protein remained in the concentrated sample.

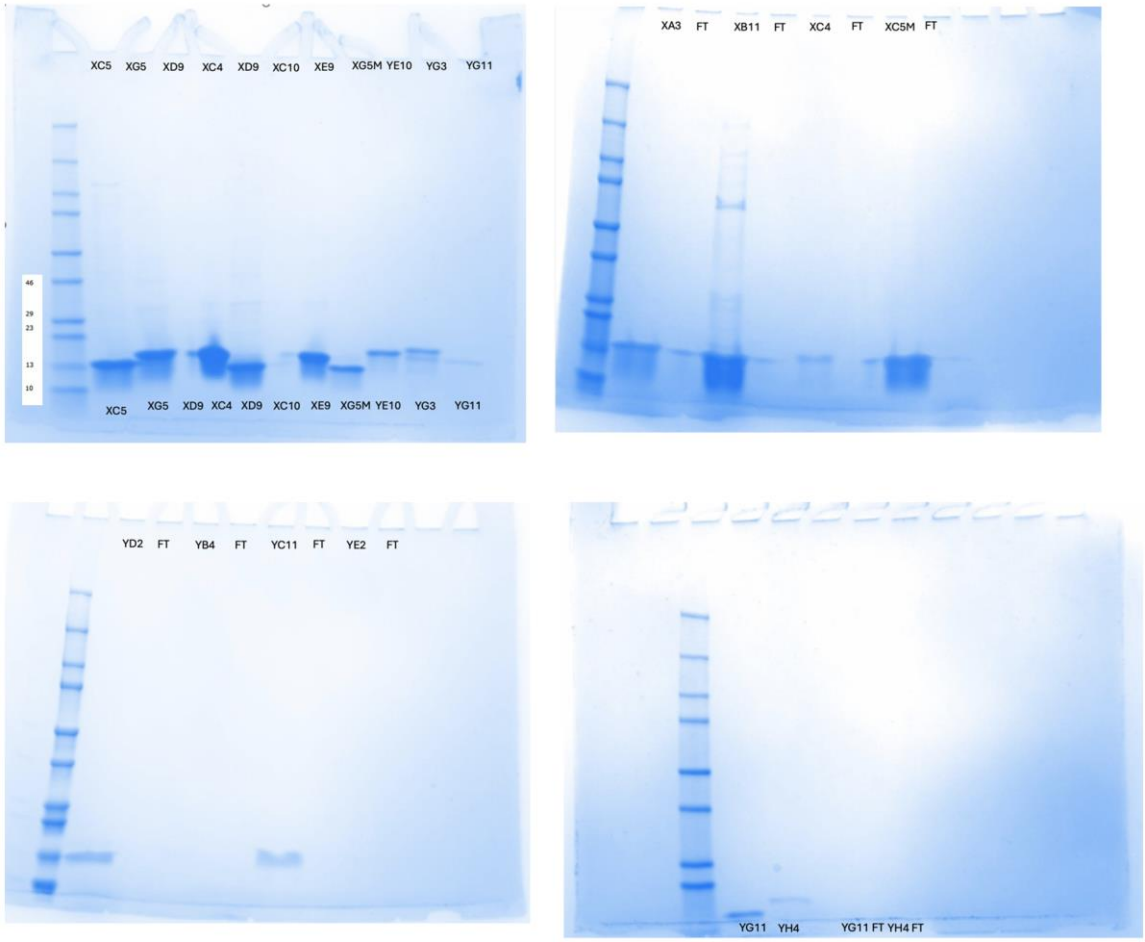

Figure 12. SDS-PAGE of purified DARPins stained with coomassie blue. Flow-through (FT) samples from 3 kDa cut-off filter are directly after the concentrated sample or marked separately.

Despite similar molecular weight of DARPins in the gel, protein bands are in notably different positions. All DARPins are roughly 15 kDa with histidine tag and bands on gel were a bit above the 13 kDa ladder. The length of the amino acid chain is the same, the

only difference comes from variable amino acids. All the protein samples were treated similarly with sodium dodecyl sulphate (SDS) before loading. Proteins are supposed to be in completely unfolded state but in case of DARPins it could be possible that some unfolded parts are still present. No glycosylation should be present from *E. coli* production. SDS binding is amino acid dependent to some extent so different amino acid composition may result in different net charge of the protein (Kielkopf et al., 2021).

3.7 Affinity measurement

DARPins were first screened at 1 µM binding concentration to select binders and conditions for more precise measurements. As expected, part of the produced DARPins bound to the target and some of them not at all. A few example graphs are shown in figure 13.

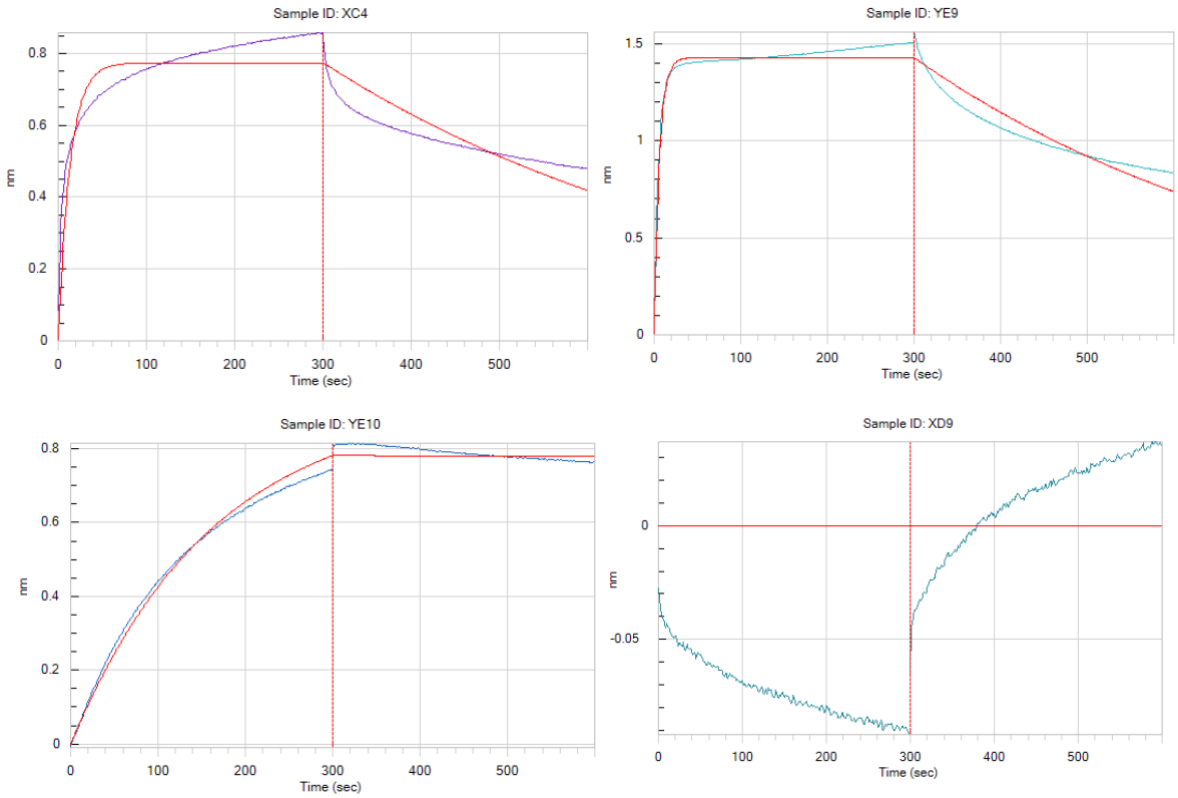

Figure 13. Affinity screening with Octet at 1000 nM concentration. Red line is fitting of 1:1 kinetic model, blue is the measurement data. First two examples (XC4, YE9) associate (0-300s) and dissociate (300-600) relatively fast. YE10 initially seemed a binder with low dissociation rate. XD9 did not show any binding behaviour.

Different binding profiles were found in more precise measurements (Figure 14). As an example, sample XC4 had the highest association rate among the measured samples. Still,

due to fast dissociation rate, affinity was much lower than the best ones.YE10 was a notable example where binding looked promising during the initial screening at but delivered unreliable results from measurement with lower binder concentrations. Total four DARPins against Y showed such uncertain binding behaviour, but none among X-binders. The affinity measurement was performed using standard buffers. It could also be tested with target specific buffers, same that were used in panning reaction.

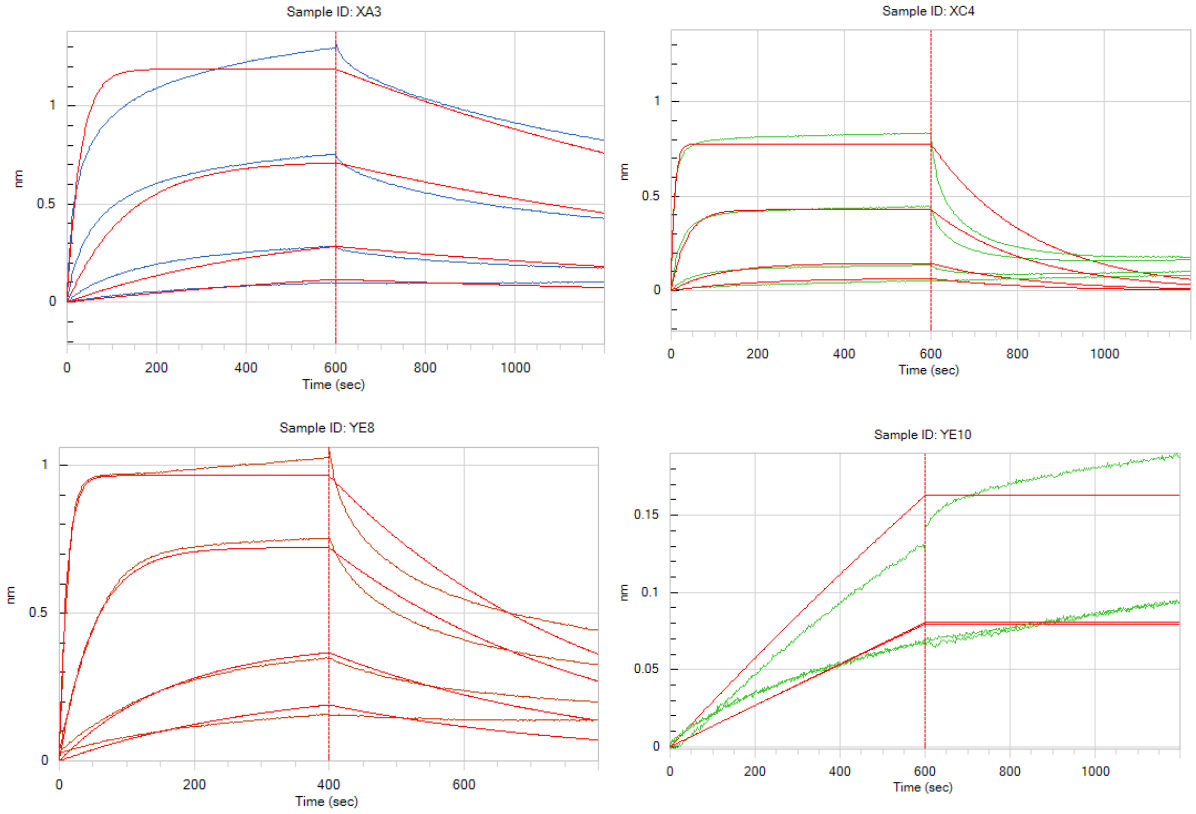

Figure 14. Affinity measurement examples. Binder concentrations 100, 20, 4, and 0.8 nM were used.

The best DARPins had nanomolar affinities and most of them were in desired level for further testing (Table 10). It needs to be noted that no affinity maturation was done. S/B ratio was expected to correlate negatively with dissociation constant KD. For all samples, Pearson correlation coefficient between S/B and KD was 0.05, excluding the ones with low signal response. For X-DARPins, the negative correlation was strong, coefficient being -0.87.

Table 10. Measured affinities from produced binders, measured with multiple binder concentrations. S/B ratio is from colony screening phage immunoassay. In last four samples,

the signal response was significantly lower than other samples and the affinity measurement may not be reliable.

Sample	S/B ratio	KD (M)	Kon (1/Ms)	Koff(1/s)	Note
XC5	207.9	8.90E-09	7.07E+04	6.29E-04	
XA3	190.0	1.14E-08	6.57E+04	7.46E-04	
XB11	158.6	3.56E-08	7.66E+04	2.73E-03	
XC10	156.1	2.27E-08	9.97E+04	2.26E-03	
XC4	205.1	1.74E-08	2.46E+05	4.29E-03	
XG5M	128.0	3.15E-08	6.50E+04	2.05E-03	
XG5	128.0	3.67E-08	2.07E+04	7.59E-04	
YE9	160.8	3.91E-09	4.92E+05	1.92E-03	
YD2	39.7	7.96E-09	1.73E+05	1.38E-03	
YH4	292.4	1.84E-08	8.36E+04	1.54E-03	
YB4	38.3	1.35E-08	1.20E+05	1.62E-03	
YE8	226.6	2.43E-08	7.66E+04	1.86E-03	
YG11	15.7	1.90E-08	9.92E+04	1.88E-03	
YE10	41.6	<1.0E-12	3.08E+03	<1.0E-07	Low response
YC11	2.1	<1.0E-12	1.95E+04	<1.0E-07	Low response
YG3	51.7	<1.0E-12	6.95E+03	<1.0E-07	Low response
YE2	42.1	<1.0E-12	7.28E+03	<1.0E-07	Low response

High off-rates and average affinities were almost expected as only one repeat module was fully randomized. If binders are considered for affinity maturation, the best approach may be to choose the DARPins with the highest on-rate as off-rate is expected to mainly improve when binding amino acids are added to DARPin. However, depending on the final application, need for epitope coverage needs to be considered as well when selecting binders.

3.8 Specificity

In almost any use case it is important that the only the intended binding reactions happen. In research, unintended binding can lead into false results. In therapeutic use, DARPin binding into other molecule than targeted, can cause unwanted side effects. For specificity, Y-binders were tested against target X (Figure 15). None of the binders showed significant increase in signal during association at 100 nM binder concentration. That indicates that cross-binding to different target is not significant.

To make the results more comprehensive, binding with higher DARPin concentration and with different antigens could have been tested. Especially testing with targets sharing structural similarities with X and Y could have been more challenging test for specificity. Negative binding result to similar target would indicate high binding specificity to just one protein.

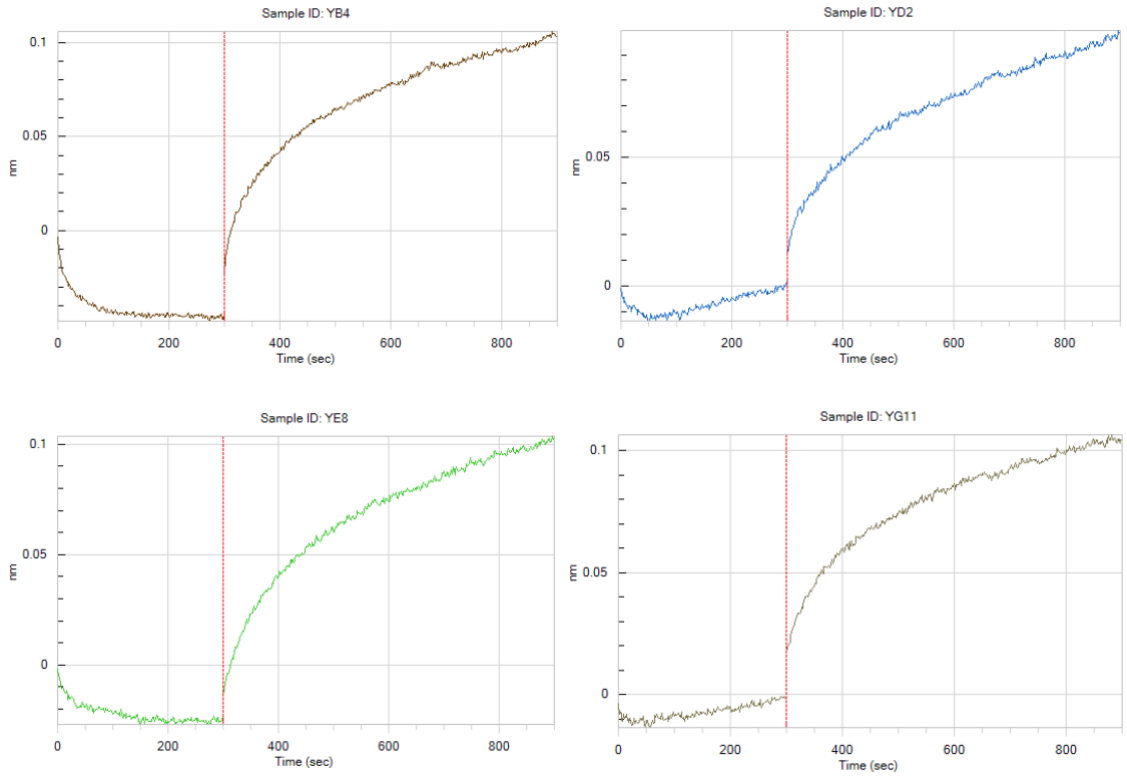

Figure 15. Cross binding of Y-DARPins to target X. Association 0 - 300 s, dissociation 300 - 900 s

3.9 Epitope binning

At first, a simple measurement was tested. Two DARPins at 500 nM concentration were sequentially bound to the immobilized target (Figure 16). If the second DARPin was bound to the different epitope, the signal would increase. For the best results, both DARPins should have high affinity in the similar level.

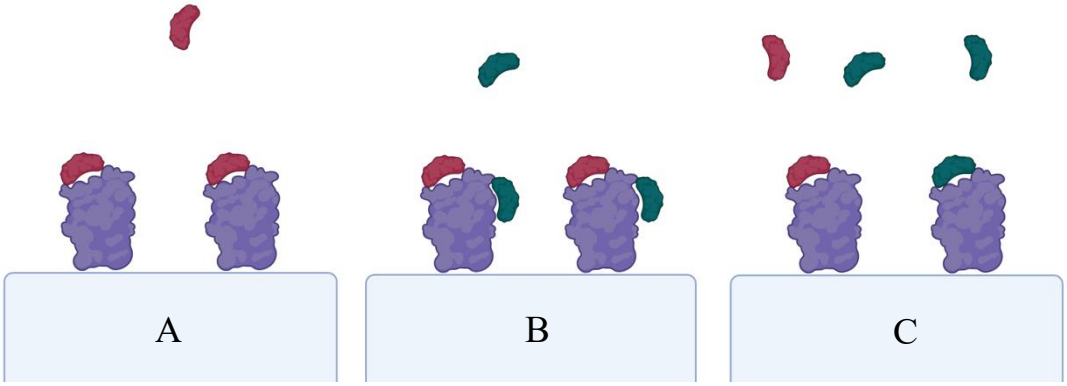

Figure 16. Illustration of epitope binning setups with BLI, target immobilised to the sensor. (A) First DARPins (red) bind into immobilized target (violet). (B) If the binding site of second DARPin (green) is different, both DARPins can bind simultaneously, increasing the signal. In case of competitive binding (C), signal is not increased. Created with biorender.com.

Most the measurements resulted in decreasing signal, making it challenging to draw a conclusion (able 11 and figure 17). Pairs (XC5, XA3) and (XC10, XB11) look the most promising for noncompetitive binding, the reactions were the only ones with increasing signal. The signal decrease can be explained by fast dissociation of the first DARPin. If the binding of the second is weak, there may be less bound DARPin in the end independent of the binding sites. If the first DARPin is weak, signal may increase even in case of competitive binding. To make the results more reliable, all the combinations could have been measured both directions, including second association with the same DARPin and with no DARPin.

Table 11. Signal change over the second association with immobilized target and two DARPins binding sequentially. Based on hypothesis, the higher the signal change (coloured green), the more likely the binding is noncompetitive.

		DARPin in second association						
		XC5	XA3	XC10	XG5M	XB11	XG5	XC4
DARPin in the first associ-ation	XC5		0.0493	-0.0708	-0.2086	-0.0962	-0.1928	
	XA3	-0.0076		-0.0812	-0.2368	-0.1209	-0.2047	
	XC10				-0.0923	0.0437	-0.0622	-0.0222

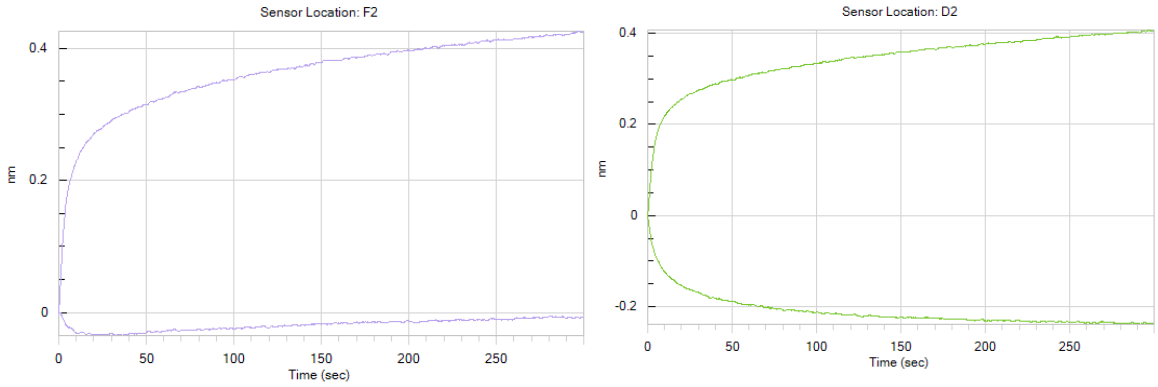

Figure 17. Example graphs of epitope binning measurements with immobilized target. Left: XA3 - XC5, right: XA3 - XG5M. First (higher line) and second association (lower line) are presented in the same time axis, both starting at 0 s. Signal in the association of the second DARPin was dominated by dissociation of the first DARPin.

To eliminate the effect of the dissociation, the second association reaction could include equal concentration of the first DARPin. Even in that case, it could be challenging to distinguish weak noncompetitive binder from strong competitive. In practice, this would consume more DARPins, which needs to be considered when planning the initial production. Increasing the production volume would be easy.

In second experiment using sandwich-type epitope binning method, the first DARPin was immobilized on amino-coupling sensor (Figure 18). Due to lack of material, only Y-binders were measured with that method. 10 nM target and 100 nM second DARPin was used. In these conditions, steady state was not reached. Free target was used as positive control, in that case no binder is competing. As negative control, the same DARPin as immobilized was competing in the second association. Another negative control was with just buffer, creating the situation where no free target is available.

Signal from epitope binning with YE9 immobilized are shown in figure 19, YE8, YE10 and YH4 were close or above the positive control. These could be potential DARPins to bind to different epitope than YE9. YB4 and YD2 were close to negative control. YB4 and YD2 with YE9 had the highest affinities among Y-DARPins. Most positive samples for noncompetitive binding with YE9 were YE10 and YH4.

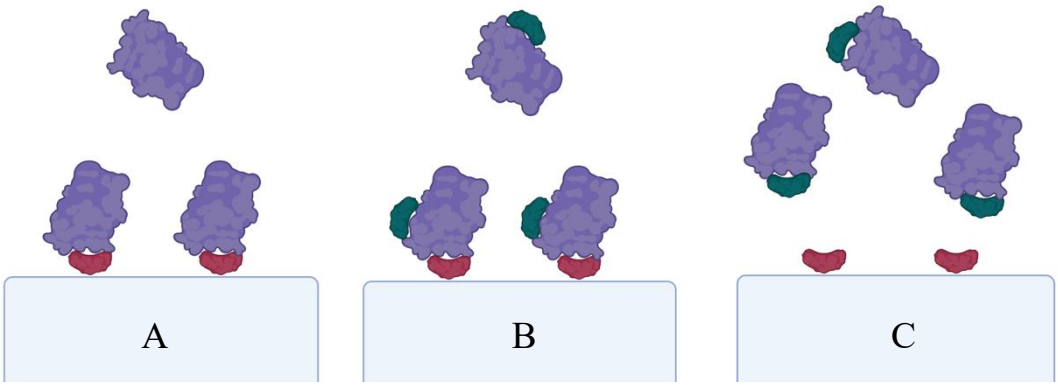

Figure 18. Epitope binning method with immobilized DARPin. (A) The target binds to immobilized DARPin, signal increases. (B) Second DARPin binding to different epitope while keeping target concentration the same, should cause a slight signal increase. (C) Alternatively, competing DARPin dissociates target protein from immobilized DARPin, leading into decreasing signal. Created with biorender.com.

When immobilizing weaker DARPin YE8 (Figure 20), contrary results were obtained regarding YE9-YE8 interaction. Signal was notably decreasing during second association with YE9, giving strong evidence for competing binding reaction. Other samples where signal was decreasing were YD2 and YB4. However, negative control (same DARPin, YE8 competing) behaved almost like positive control (with no competing binder). That questions the reliability of the used method. The binders that seemed to have a different epitope than immobilized YE8 and YE9 were YE10, YH4 and YE8. At the same time, these had the weakest affinities among the tested group. As YE8 cannot be noncompetitive with itself, the challenge remains the same with this method, how to distinguish weak competitive binding from noncompetitive. Full testing with all permutations would still be needed to validate the results.

No clear example was found where two DARPins would bind to different epitopes. Neither is the conclusion that all the measured DARPins would bind to the same site in the target. Such case is unexpected as target should have multiple possible binding sites available. One possibility is competitive binding even without competitive binding. Another way to verify two different binding sites would be to create double-DARPin from each combination with a linker. If the avidity of the combination is higher than the affinity of an individual binder, there would be evidence that two DARPins bind to different epitopes.

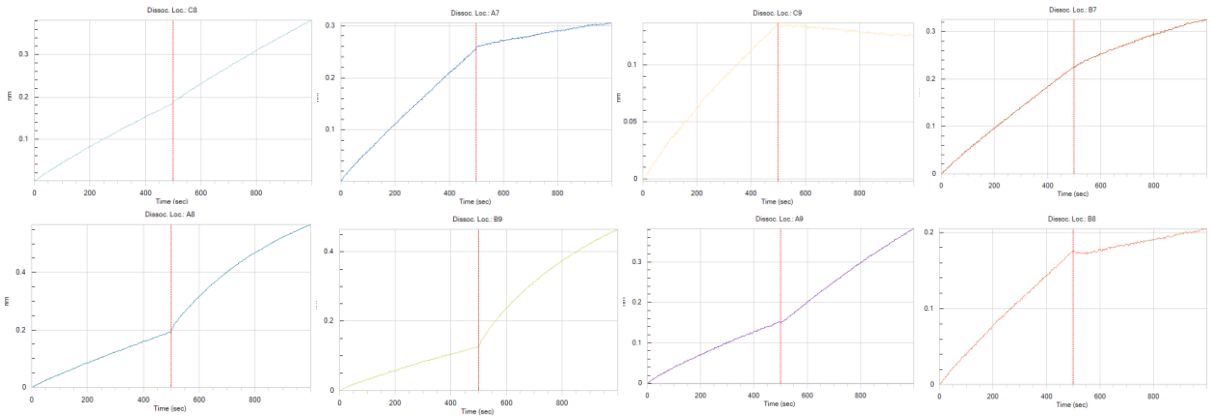

Figure 19. Epitope binning data with DARPin YE9 immobilized. Top from left: positive control, target with no competing binder; negative control, YE9 competing in second association negative control, no target in second association; YD2. Bottom row from left to right: YE8, YE10, YH4, YB4

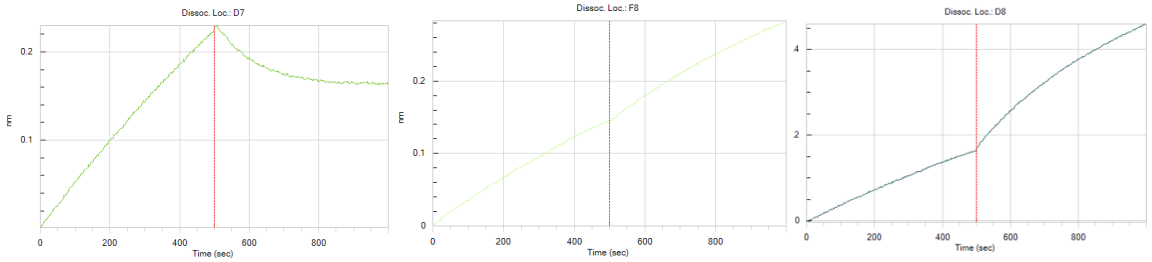

Figure 20. Epitope binning with YE8 immobilized. From left: YE9; positive control (only target); negative control (YE8).

3.10 General discussion

From general point of view, the results were quite expected. Binders with acceptable affinities were found against both targets. Epitope binning could not be confirmed successful and would require further research. In this section, improvements to the methods used in research are suggested. Also, different approaches in the whole process are considered.

While phage display is a robust technology for biopanning, ribosome or DNA-based display system would have a capacity to handle larger number of clones. Utilizing that in biopanning could increase the coverage of the theoretical diversity of the library and increase the probability of enriching the best binders. Moreover, with cell free display, there is one expressed protein per complex. That eliminates the multivalent binding that makes binding strength dependent on the display level and is likely present in phage display.

Based on sequencing, binder enrichment was not strong. It means that the diversity in the output was high, possibly leading into situation where some of the strongest binders were not characterized due to large number of weaker binders. Screening with phage immunoassay did not seem to be necessarily accurate to predict the affinity of the binder. For these reasons, continuing the characterization with larger set of binders from colony screening could potentially present new even higher affinity binders. It could be possible to do cloning into production vector in 96 plate form to speed up the process.

The enrichment itself could be improved with additional panning rounds. Another approach would be NGS of the whole panning output instead of colony picking and screening. Instead of S/B from phage immunoassay, characterized binders would be chosen based on the frequency of repetition of sequence in the panning output. If functional, that approach could be less labour-intensive compared to phage immunoassay and more sensitive for less advanced binder enrichment.

Relatively low hit rate on round 4 could have affected the creation of the twin-DARPin library. It is possible that limited coverage of all combinations in the combination library and low hit rate resulted in the situation where selected twin-DARPins only contain one unit responsible for binding. Stronger binding compared to individual would require two DARPins bind to different epitopes in DARPin. It is also possible that the binding is biased towards certain epitope. That would further decrease the possibility of having DARPins binding to two epitopes.

In current approach, after selections, binders were produced, screened as soluble proteins, then measured for more precise affinity, and lastly epitope binning was attempted. While clear results were not got from epitope binning, the method optimization could improve the outcome. If rational design of multispecific binder is the main objective, computational prediction of binding site could be an option. One pipeline (Radom et al., 2019) only requires DARPin sequence and target structure as input and predicts the structure of the binding complex, revealing the epitope for each DARPin. Recent advancements in AI-based protein structure prediction tools such as Alpha Fold 2 (Jumper et al., 2021), could eliminate the need for determining the protein structure with traditional methods such as X-ray crystallography. That would enable using the pipeline with proteins, structures of which were not available or were not even possible to determine with traditional methods.

4 Conclusions

The aims of the study were achieved in most parts, providing strong evidence for the functionality of the DARPin library against different targets. Despite some target related challenges and using special biopanning conditions, binders were found against both the targets. Characterization of DARPins was successful except from epitope binning. There was still room for improvement if the pipeline is reused with other targets. Most importantly, binder enrichment and epitope binning could be enhanced.

Continuation from this study could include screening for functional properties of the binders. If stronger binding is needed, found binders could be affinity maturated. Larger number of DARPins from panning round four could be tested as in this study, only a fraction of them were characterized.

Even as such, the work was a proof of concept for using the DARPin library as a platform for early-stage drug discovery even against potentially challenging targets. Moreover, well-behaving binder with trivial modification into stabile multi-specifics can be assumed to have multiple potential use cases. Validating the functionality of the library opens possibilities to use it for binder selection for many types of research, diagnostic or therapeutic purposes.

References

ACTIV-3/TICO Study Group. (2022). Efficacy and Safety of Ensovibep for Adults Hospitalized With COVID-19. *Annals of Internal Medicine*. https://doi.org/10.7326/M22-1503

Allergan. (2020). *Safety and Efficacy of Abicipar Pegol (AGN-150998) in Patients With Neovascular Age-related Macular Degeneration (CEDAR Study)* (Clinical Trial Registration NCT02462928). clinicaltrials.gov. https://clinicaltrials.gov/study/NCT02462928

Amstutz, P., Binz, H. K., Parizek, P., Stumpp, M. T., Kohl, A., Grütter, M. G., Forrer, P., & Plückthun, A. (2005). Intracellular kinase inhibitors selected from combinatorial libraries of designed ankyrin repeat proteins. *The Journal of Biological Chemistry*, *280*(26), 24715–24722. https://doi.org/10.1074/jbc.M501746200

Baird, R. D., Linossi, C., Middleton, M., Lord, S., Harris, A., Rodón, J., Zitt, C., Fiedler, U., Dawson, K. M., Leupin, N., Stumpp, M. T., Harstrick, A., Azaro, A., Fischer, S., & Omlin, A. (2021). First-in-Human Phase I Study of MP0250, a First-in-Class DARPin Drug Candidate Targeting VEGF and HGF, in Patients With Advanced Solid Tumors. *Journal of Clinical Oncology*. https://doi.org/10.1200/JCO.20.00596

Best, R. L., LaPointe, N. E., Azarenko, O., Miller, H., Genualdi, C., Chih, S., Shen, B.-Q., Jordan, M. A., Wilson, L., Feinstein, S. C., & Stagg, N. J. (2021). Microtubule and tubulin binding and regulation of microtubule dynamics by the antibody drug conjugate (ADC) payload, monomethyl auristatin E (MMAE): Mechanistic insights into MMAE ADC peripheral neuropathy. *Toxicology and Applied Pharmacology*, *421*, 115534. https://doi.org/10.1016/j.taap.2021.115534

Binz, H. K., Bakker, T. R., Phillips, D. J., Cornelius, A., Zitt, C., Göttler, T., Sigrist, G., Fiedler, U., Ekawardhani, S., Dolado, I., Saliba, J. A., Tresch, G., Proba, K., & Stumpp, M. T. (2017). Design and characterization of MP0250, a tri-specific anti-HGF/anti-VEGF DARPin® drug candidate. *mAbs*, *9*(8), 1262–1269. https://doi.org/10.1080/19420862.2017.1305529

Blass, B. E. (2015). *Basic principles of drug discovery and development* (Second edition.). Academic Press.

Cary, D. R., Ohuchi, M., Reid, P. C., & Masuya, K. (2017). Constrained Peptides in Drug Discovery and Development. *Journal of Synthetic Organic Chemistry, Japan*, *75*(11), 1171–1178. https://doi.org/10.5059/yukigoseikyokaishi.75.1171

Durie, B. G. M., Harousseau, J.-L., Miguel, J. S., Bladé, J., Barlogie, B., Anderson, K., Gertz, M., Dimopoulos, M., Westin, J., Sonneveld, P., Ludwig, H., Gahrton, G., Beksac, M., Crowley, J., Belch, A., Boccadaro, M., Turesson, I., Joshua, D., Vesole, D., … Rajkumar, S. V. (2006). International uniform response criteria for multiple myeloma. *Leukemia*, *20*(9), 1467–1473. https://doi.org/10.1038/sj.leu.2404284

Esfandiari, A., Cassidy, S., & Webster, R. M. (2022). Bispecific antibodies in oncology. *Nature Reviews Drug Discovery*, *21*(6), 411–412. https://doi.org/10.1038/d41573-022-00040-2

Fiedler, U., Metz, C., Zitt, C., Bessey, R., Béhé, M., Blanc, A., Schibli, R., Dolado, I., Herbst, J., Dawson, K., & Kiemle-Kallee, J. (2017). Abstract P4-21-18: Pre-clinical antitumor activity, tumor localization, and pharmacokinetics of MP0274, an apoptosis inducing, biparatopic HER2-targeting DARPin®. *Cancer Research*, *77*(4_Supplement), P4-21–18. https://doi.org/10.1158/1538-7445.SABCS16-P4-21-18

Fischer, S., Götze, T. O., Omlin, A., Baird, R. D., Dawson, K. M., Zitt, C., Arany, Z., Tresch, G., Fiedler, U., Jeger, S., Fung, S., Legenne, P., Leupin, N., Schneeweiss, A., & Fremd, C. (2022). A Case of Sustained Tumor Regression With MP0274, a Novel DARPin Therapeutic Targeting Human Epidermal Growth Factor Receptor 2 Signaling, in Metastatic Human Epidermal Growth Factor Receptor 2–Positive Breast Cancer After Prior Trastuzumab and Pertuzumab. *JCO Precision Oncology*, *6*, e2200006. https://doi.org/10.1200/PO.22.00006

FONTAINE, S., BOSSHART, A., Schlereth, B., Steiner, D., & Walser, M. (2023). *Designed repeat domains with dual binding specificity and their use* (World Intellectual Property Organization Patent WO2023110983A1). https://patents.google.com/patent/WO2023110983A1/en

Forrer, P., Stumpp, M. T., Binz, H. K., & Plückthun, A. (2003). A novel strategy to design binding molecules harnessing the modular nature of repeat proteins. *FEBS Letters*, *539*(1–3), 2–6. https://doi.org/10.1016/S0014-5793(03)00177-7

Gomez-Roca, C. A., Korakis, I., Gort, E. H., Winter, H. A. M. D., Stojcheva, N., Stavropoulou, V., Krieg, J., Baverel, P., Fernandez, E., Florescu, A. M., Stumpp, M. T., Legenne, P., & Cassier, P. A. (2024). Effect of MP0317, a FAP x CD40 DARPin, on safety profile and tumor-localized CD40 activation in a phase 1 study in patients with advanced solid tumors. *Journal of Clinical Oncology*. https://doi.org/10.1200/JCO.2024.42.16_suppl.2573

Goulet, D. R., & Atkins, W. M. (2020). Considerations for the Design of Antibody-Based Therapeutics. *Journal of Pharmaceutical Sciences*, *109*(1), 74–103. https://doi.org/10.1016/j.xphs.2019.05.031

Hanes, J., & Plückthun, A. (1997). In vitro selection and evolution of functional proteins by using ribosome display. *Proceedings of the National Academy of Sciences*, *94*(10), 4937–4942. https://doi.org/10.1073/pnas.94.10.4937

Ioannou, K., Ragusa, S., Roquette, J., Florescu, A., Gachechiladze, M., Müller, E., Martinez-Gomez, J. M., Barsin, S., Jetzer, S., Rigamonti, N., Domke, C., Lekishvili, T., Rommel, K., Tosevski, I., Goubier, A., Legenne, P., Kirkin, V., Levesque, M., Ji, H., & Kenefeck, R. (2021). Abstract 1733: MP0317, a CD40xFAP targeting multi-specific DARPin® therapeutic, drives immune activation and reverts myeloid-mediated T-cell suppression in vitro and ex vivo. *Cancer Research*, *81*(13_Supplement), 1733. https://doi.org/10.1158/1538-7445.AM2021-1733

Ji, X., Nielsen, A. L., & Heinis, C. (2024). Cyclic Peptides for Drug Development. *Angewandte Chemie International Edition*, *63*(3), e202308251. https://doi.org/10.1002/anie.202308251

Jin, B., Odongo, S., Radwanska, M., & Magez, S. (2023). NANOBODIES®: A Review of Diagnostic and Therapeutic Applications. *International Journal of Molecular Sciences*, *24*(6), Article 6. https://doi.org/10.3390/ijms24065994

Johnson, L. A., & June, C. H. (2016). Driving gene-engineered T cell immunotherapy of cancer. *Cell Research*, *27*(1), 38. https://doi.org/10.1038/cr.2016.154

Jongen-Lavrencic, M., Pabst, T., Bories, P., Griškevičius, L., Huls, G., de Leeuw, D. C., Boettcher, S., Pigneux, A., Boissel, N., Dymkowska, M., Andrieu, C., Schönborn-Kellenberger, O., Baverel, P. G., Arany, Z., Fernandez, E., Florescu, A.-M., Sanderson, M. P., Goubier, A., Kirkin, V., … Subklewe, M. (2024). MP0533 (CD33 x CD123 x CD70 x CD3), a Tetra-Specific CD3-Engaging Darpin for the Treatment of Patients with Relapsed/Refractory AML or

MDS/AML: Results of an Ongoing Phase 1/2a Study. *Blood*, *144*, 2881. https://doi.org/10.1182/blood-2024-199211

Jumper, J., Evans, R., Pritzel, A., Green, T., Figurnov, M., Ronneberger, O., Tunyasuvunakool, K., Bates, R., Žídek, A., Potapenko, A., Bridgland, A., Meyer, C., Kohl, S. A. A., Ballard, A. J., Cowie, A., Romera-Paredes, B., Nikolov, S., Jain, R., Adler, J., … Hassabis, D. (2021). Highly accurate protein structure prediction with AlphaFold. *Nature*, *596*(7873), 583–589. https://doi.org/10.1038/s41586-021-03819-2

Kamata-Sakurai, M., Narita, Y., Hori, Y., Nemoto, T., Uchikawa, R., Honda, M., Hironiwa, N., Taniguchi, K., Shida-Kawazoe, M., Metsugi, S., Miyazaki, T., Wada, N. A., Ohte, Y., Shimizu, S., Mikami, H., Tachibana, T., Ono, N., Adachi, K., Sakiyama, T., … Igawa, T. (2021). Antibody to CD137 Activated by Extracellular Adenosine Triphosphate Is Tumor Selective and Broadly Effective In Vivo without Systemic Immune Activation. *Cancer Discovery*, *11*(1), 158–175. https://doi.org/10.1158/2159-8290.CD-20-0328

Karsten, L., Janson, N., Joncour, V. L., Alam, S., Müller, B., Ramanathan, J. T., Laakkonen, P., Sewald, N., & Müller, K. M. (2022). Bivalent EGFR-Targeting DARPin-MMAE Conjugates. *International Journal of Molecular Sciences*, *23*(5), 2468. https://doi.org/10.3390/ijms23052468

Khurana, R. N., Kunimoto, D., Yoon, Y. H., Wykoff, C. C., Chang, A., Maturi, R. K., Agostini, H., Souied, E., Chow, D. R., Lotery, A. J., Ohji, M., Bandello, F., Belfort, R., Li, X.-Y., Jiao, J., Le, G., Kim, K., Schmidt, W., & Hashad, Y. (2021). Two-Year Results of the Phase 3 Randomized Controlled Study of Abicipar in Neovascular Age-Related Macular Degeneration. *Ophthalmology*, *128*(7), 1027–1038. https://doi.org/10.1016/j.ophtha.2020.11.017

Kielkopf, C. L., Bauer, W., & Urbatsch, I. L. (2021). Sodium Dodecyl Sulfate–Polyacrylamide Gel Electrophoresis of Proteins. *Cold Spring Harbor Protocols*, *2021*(12), pdb.prot102228. https://doi.org/10.1101/pdb.prot102228

Kim, B., Eggel, A., Tarchevskaya, S. S., Vogel, M., Prinz, H., & Jardetzky, T. S. (2012). Accelerated Disassembly of IgE:Receptor Complexes by a Disruptive Macromolecular Inhibitor. *Nature*, *491*(7425), 613. https://doi.org/10.1038/nature11546

Knop, S., Szarejko, M., Grząśko, N., Bringhen, S., Trautmann-Grill, K., Jurczyszyn, A., Vacca, A., Khandanpour, C., Gamberi, B., Pour, L., Iversen, K. F., Stumpp, M.

T., Suter, C., Dawson, K. M., Zitt, C., Legenne, P., Stavropoulou, V., Fey, M. F., Leupin, N., & Goldschmidt, H. (2024). A phase 1b/2 study evaluating efficacy and safety of MP0250, a designed ankyrin repeat protein (DARPin) simultaneously targeting vascular endothelial growth factor (VEGF) and hepatocyte growth factor (HGF), in combination with bortezomib and dexamethasone, in patients with relapsed or refractory multiple myeloma. *eJHaem*, *5*(5), 940–950. https://doi.org/10.1002/jha2.968

Könning, D., & Kolmar, H. (2018). Beyond antibody engineering: Directed evolution of alternative binding scaffolds and enzymes using yeast surface display. *Microbial Cell Factories*, *17*(1), 32. https://doi.org/10.1186/s12934-018-0881-3

Kulmala, A., Lappalainen, M., Lamminmäki, U., & Huovinen, T. (2022). Synonymous Codons and Hydrophobicity Optimization of Post-translational Signal Peptide PelB Increase Phage Display Efficiency of DARPins. *ACS Synthetic Biology*, *11*(10), 3174–3181. https://doi.org/10.1021/acssynbio.2c00260

Kummer, L., Hsu, C.-W., Dagliyan, O., MacNevin, C., Kaufholz, M., Zimmermann, B., Dokholyan, N. V., Hahn, K. M., & Plückthun, A. (2013). Knowledge-based design of a biosensor to quantify localized ERK activation in living cells. *Chemistry & Biology*, *20*(6), 847–856. https://doi.org/10.1016/j.chembiol.2013.04.016

Kurz, M., Gu, K., Al-Gawari, A., & Lohse, P. A. (2001). cDNA–Protein Fusions: Covalent Protein–Gene Conjugates for the In Vitro Selection of Peptides and Proteins. *ChemBioChem*, *2*(9), 666–672. https://doi.org/10.1002/1439-7633(20010903)2:9<666::AID-CBIC666>3.0.CO;2-#

Lehmusvuori, A., Manninen, J., Huovinen, T., Soukka, T., & Lamminmäki, U. (2012). Homogenous M13 Bacteriophage Quantification Assay Using Switchable Lanthanide Fluorescence Probes. *BioTechniques*, *53*, 301–303. https://doi.org/10.2144/0000113954

Li, J., Mahajan, A., & Tsai, M.-D. (2006). Ankyrin Repeat: A Unique Motif Mediating Protein−Protein Interactions. *Biochemistry*, *45*(51), 15168–15178. https://doi.org/10.1021/bi062188q

Lizak, C., Bosshart, A., Wullschleger, S., Behe, M., Blanc, A., Imobersteg, S., Neculcea, A., Blunschi, J., Abduli, L., Schütz, S., Wolter, J., Reichen, C., Croset, A., Villa, A., Goubier, A., Legenne, P., Schibli, R., & Steiner, D. (2023). DARPin platform for the development of powerful targeting agents for

radioligand therapy. *Journal of Nuclear Medicine*, *64*(supplement 1), P246–P246.

Mann, H. B., & Whitney, D. R. (1947). On a Test of Whether one of Two Random Variables is Stochastically Larger than the Other. *The Annals of Mathematical Statistics*, *18*(1), 50–60.

Molecular Partners. (2022, April 26). *Molecular Partners to Regain Global Rights for MP0310 from Amgen*. GlobeNewswire News Room. https://www.globenewswire.com/news-release/2022/04/26/2429624/0/en/Molecular-Partners-to-Regain-Global-Rights-for-MP0310-from-Amgen.html

Molecular Partners AG. (2022). *A First-In-Human, Single-Arm, Multi-Center, Open-Label, Repeated-Dose, Dose-Escalation Study of MP0310 in Patients With Advanced Solid Tumors* (Clinical Trial Registration NCT04049903). clinicaltrials.gov. https://clinicaltrials.gov/study/NCT04049903

Monoclonal Antibody Therapeutics Market Size And Global Industry Forecast 2029. (2024, April 1). MarketsandMarkets. https://www.marketsandmarkets.com/Market-Reports/monoclonal-antibody-mabs-therapeutics-market-115323820.html

Mozhaev, V., Berezin, I., Martinek, K., & Nosoh, Y. (1988). Structure-Stability Relationship in Proteins: Fundamental Tasks and Strategy for the Development of Stabilized Enzyme Catalysts for Biotechnolog. *Critical Reviews in Biochemistry and Molecular Biology - CRIT REV BIOCHEM MOLEC BIOL*, *23*, 235–281. https://doi.org/10.3109/10409238809088225

Mullard, A. (2022). FDA approves second BCMA-targeted CAR-T cell therapy. *Nature Reviews Drug Discovery*, *21*(4), 249–249. https://doi.org/10.1038/d41573-022-00048-8

N, R., N, V., C, D., S, B., S, J., O, A., R, B., T, L., F, M., M, G., M, B., V, L., & Pa, T. (2022). A Multispecific Anti-CD40 DARPin Construct Induces Tumor-Selective CD40 Activation and Tumor Regression. *Cancer Immunology Research*, *10*(5). https://doi.org/10.1158/2326-6066.CIR-21-0553

Nix, M. A., & Wiita, A. P. (2024). Alternative target recognition elements for chimeric antigen receptor (CAR) T cells: Beyond standard antibody fragments. *Cytotherapy*, *26*(7), 729–738. https://doi.org/10.1016/j.jcyt.2024.02.024

Orano Med. (2024, November 6). *Molecular Partners and Orano Med Share Positive Preclinical Data of their DLL3-Targeting Radio-DARPin Therapy (RDT) Candidate MP0712 at SNMMI 2024*. Medical.Orano.Group. https://www.oranomed.com/en/resources/news/2024/molecular-partners-and-orano-med-share-positive-preclinical-data-of-their-dll3-targeting-radio-darpin-therapy-rdt-candidate-mp0712-at-snmmi-2024

Owen, D. H., Giffin, M. J., Bailis, J. M., Smit, M.-A. D., Carbone, D. P., & He, K. (2019). DLL3: An emerging target in small cell lung cancer. *Journal of Hematology & Oncology*, *12*(1), 61. https://doi.org/10.1186/s13045-019-0745-2

Park, S. J., & Cochran, J. R. (2010). *Protein engineering and design*. CRC Press.

Patasic, L., Seifried, J., Bezler, V., Kaljanac, M., Schneider, I. C., Schmitz, H., Tondera, C., Hartmann, J., Hombach, A., Buchholz, C. J., Abken, H., König, R., & Cichutek, K. (2020). Designed Ankyrin Repeat Protein (DARPin) to target chimeric antigen receptor (CAR)-redirected T cells towards CD4+ T cells to reduce the latent HIV+ cell reservoir. *Medical Microbiology and Immunology*, *209*(6), 681–691. https://doi.org/10.1007/s00430-020-00692-0

Pennington, L. F., Gasser, P., Brigger, D., Guntern, P., Eggel, A., & Jardetzky, T. S. (2021). Structure-guided design of ultrapotent disruptive IgE inhibitors to rapidly terminate acute allergic reactions. *The Journal of Allergy and Clinical Immunology*, *148*(4), 1049. https://doi.org/10.1016/j.jaci.2021.03.050

Piantadosi, S. (2024). *Clinical Trials: A Methodologic Perspective*. John Wiley & Sons.

Plückthun, A. (2015). Designed Ankyrin Repeat Proteins (DARPins): Binding Proteins for Research, Diagnostics, and Therapy. *Annual Review of Pharmacology and Toxicology*, *55*(Volume 55, 2015), 489–511. https://doi.org/10.1146/annurev-pharmtox-010611-134654

Radom, F., Paci, E., & Plückthun, A. (2019). Computational Modeling of Designed Ankyrin Repeat Protein Complexes with Their Targets. *Journal of Molecular Biology*, *431*(15), 2852–2868. https://doi.org/10.1016/j.jmb.2019.05.005

Rothenberger, S., Hurdiss, D. L., Walser, M., Malvezzi, F., Mayor, J., Ryter, S., Moreno, H., Liechti, N., Bosshart, A., Iss, C., Calabro, V., Cornelius, A., Hospodarsch, T., Neculcea, A., Looser, T., Schlegel, A., Fontaine, S., Villemagne, D., Paladino, M., … Trimpert, J. (2021). *Multi-specific DARPin(R) therapeutics demonstrate very high potency against mutated SARS-CoV-2 variants in vitro*. https://biorxiv.org/cgi/content/short/2021.02.03.429164

Schütz, M., Batyuk, A., Klenk, C., Kummer, L., de Picciotto, S., Gülbakan, B., Wu, Y., Newby, G. A., Zosel, F., Schöppe, J., Sedlák, E., Mittl, P. R. E., Zenobi, R., Wittrup, K. D., & Plückthun, A. (2016). Generation of Fluorogen-Activating Designed Ankyrin Repeat Proteins (FADAs) as Versatile Sensor Tools. *Journal of Molecular Biology*, *428*(6), 1272–1289. https://doi.org/10.1016/j.jmb.2016.01.017

Scipy/scipy/stats/_mannwhitneyu.py at v1.14.1 · scipy/scipy. (n.d.). GitHub. Retrieved 3 January 2025, from https://github.com/scipy/scipy/blob/v1.14.1/scipy/stats/_mannwhitneyu.py

Sennhauser, G., & Grütter, M. G. (2008). Chaperone-Assisted Crystallography with DARPins. *Structure*, *16*(10), 1443–1453. https://doi.org/10.1016/j.str.2008.08.010

Shastry, M., Gupta, A., Chandarlapaty, S., Young, M., Powles, T., & Hamilton, E. (2023). Rise of Antibody-Drug Conjugates: The Present and Future. *American Society of Clinical Oncology Educational Book*, *43*, e390094. https://doi.org/10.1200/EDBK_390094

Simeon, R. A., Zeng, Y., Chonira, V., Aguirre, A. M., Lasagna, M., Baloh, M., Sorg, J. A., Tommos, C., & Chen, Z. (2021). Protease-stable DARPins as promising oral therapeutics. *Protein Engineering, Design and Selection*, *34*, gzab028. https://doi.org/10.1093/protein/gzab028

Song, X., Chen, X., Liu, L., Yi, Y., Tian, H., Gao, X., & Yao, W. (2019). Efficient evolved antibody mimetic designed ankyrin repeat proteins against programmed death-ligand 1 on *E. coli* surface display. *Biochemical Engineering Journal*, *148*, 1–8. https://doi.org/10.1016/j.bej.2019.04.011

Steeghs, N., Gomez-Roca, C. A., Korakis, I., Gort, E. H., De Winter, H. A. M., Stojcheva, N., Stavropoulou, V., Krieg, J., Baverel, P., Fernandez, E., Florescu, A. M., Stumpp, M. T., Legenne, P., & Cassier, P. A. (2024). Effect of MP0317, a FAP x CD40 DARPin, on safety profile and tumor-localized CD40 activation in a phase 1 study in patients with advanced solid tumors. *Journal of Clinical Oncology*, *42*(16_suppl), 2573–2573. https://doi.org/10.1200/JCO.2024.42.16_suppl.2573

Steiner, D., Forrer, P., & Plückthun, A. (2008). Efficient Selection of DARPins with Sub-nanomolar Affinities using SRP Phage Display. *Journal of Molecular Biology*, *382*(5), 1211–1227. https://doi.org/10.1016/j.jmb.2008.07.085

Stumpp, M. (2021). *Ensovibep, a novel trispecific DARPin candidate that protects against SARS-CoV-2 variant*. https://doi.org/10.21203/rs.3.rs-1170399/v1

Stumpp, M. T., Binz, H. K., & Amstutz, P. (2008). DARPins: A new generation of protein therapeutics. *Drug Discovery Today*, *13*(15), 695–701. https://doi.org/10.1016/j.drudis.2008.04.013

Stumpp, M. T., Dawson, K. M., & Binz, H. K. (2020). Beyond Antibodies: The DARPin® Drug Platform. *BioDrugs*, *34*(4), 423–433. https://doi.org/10.1007/s40259-020-00429-8

Tabuchi, I., Soramoto, S., Nemoto, N., & Husimi, Y. (2001). An in vitro DNA virus for in vitro protein evolution. *FEBS Letters*, *508*(3), 309–312. https://doi.org/10.1016/S0014-5793(01)03075-7

Verdino, P., Atwell, S., & Demarest, S. J. (2018). Emerging trends in bispecific antibody and scaffold protein therapeutics. *Current Opinion in Chemical Engineering*, *19*, 107–123. https://doi.org/10.1016/j.coche.2018.01.004

Verdurmen, W. P. R., Luginbühl, M., Honegger, A., & Plückthun, A. (2015). Efficient cell-specific uptake of binding proteins into the cytoplasm through engineered modular transport systems. *Journal of Controlled Release*, *200*, 13–22. https://doi.org/10.1016/j.jconrel.2014.12.019

Vorobyeva, A., Schulga, A., Konovalova, E., Güler, R., Mitran, B., Garousi, J., Rinne, S., Löfblom, J., Orlova, A., Deyev, S., & Tolmachev, V. (2019). Comparison of tumor-targeting properties of directly and indirectly radioiodinated designed ankyrin repeat protein (DARPin) G3 variants for molecular imaging of HER2. *International Journal of Oncology*, *54*(4), 1209–1220. https://doi.org/10.3892/ijo.2019.4712

Vugmeyster, Y., Xu, X., Theil, F.-P., Khawli, L. A., & Leach, M. W. (2012). Pharmacokinetics and toxicology of therapeutic proteins: Advances and challenges. *World Journal of Biological Chemistry*, *3*(4), 73–92. https://doi.org/10.4331/wjbc.v3.i4.73

Wyatt, P. G., Gilbert, I. H., Read, K. D., & Fairlamb, A. H. (2011). Target Validation: Linking Target and Chemical Properties to Desired Product Profile. *Current Topics in Medicinal Chemistry*, *11*(10), 1275–1283. https://doi.org/10.2174/156802611795429185

Zeng, Y., Woolley, M., Chockalingam, K., Thomas, B., Arora, S., Hook, M., & Chen, Z. (2023). Click display: A rapid and efficient in vitro protein display method for

directed evolution. *Nucleic Acids Research*, *51*(16), e89. https://doi.org/10.1093/nar/gkad643

Zhang, Y., Wang, Y., Uslu, S., Venkatachalapathy, S., Rashidian, M., Schaefer, J. V., Plückthun, A., & Distefano, M. D. (2022). Enzymatic Construction of DARPin-Based Targeted Delivery Systems Using Protein Farnesyltransferase and a Capture and Release Strategy. *International Journal of Molecular Sciences*, *23*(19), Article 19. https://doi.org/10.3390/ijms231911537

Zhou, C., Jacobsen, F. W., Cai, L., Chen, Q., & Shen, D. (2010). Development of a novel mammalian cell surface antibody display platform. *mAbs*, *2*(5), 508–518. https://doi.org/10.4161/mabs.2.5.12970